Adama Science and Technology University

School of Electrical Engineering and Computing

Department of Electrical and Computer Engineering

Design and Modeling of off-grid DC Micro-grid for DC Homes: Case Study of Lake Ziway Highland (Tullu Gudo Island)

A thesis submitted to adama science and technology university school of engineering, adama science and technology university

In partial fulfillment of the requirement for the degree of MASTERS OF SCIENCE IN ELECTRICAL ENGINEERING (ELECTRICAL POWER ENGINEERING)

By: Mati Oljira Regassa

June, 2018
Adama- Ethiopia

Adama Science and Technology University

School of Electrical Engineering and Computing

Department of Electrical and Computer Engineering

Design and Modeling of off-grid DC Micro-grid for DC Homes: Case Study of Lake Ziway Highland (Tullu Gudo Island)

A thesis submitted to adama science and technology university school of engineering, adama science and technology university

In partial fulfillment of the requirement for the degree of MASTERS OF SCIENCE IN ELECTRICAL ENGINEERING (ELECTRICAL POWER ENGINEERING)

By: Mati Oljira Regassa

Advisor: Dr.-Ing Getachew Biru Worku

June, 2018
Adama- Ethiopia

Approval of Board of Examiners

We, the undersigned, members of the Board of Examiners of the final open defense. By Mati Oljira have read and evaluated his thesis entitled: **"Design and Modeling of off-grid DC Micro-grid for DC Homes: Case Study of Lake Ziway Highland (Tullu Gudo Island)"** and examined the candidate. This is, therefore, to certify that the thesis has been accepted in partial fulfillment of the requirement of the **Degree of Masters of Science in Electrical Power Engineering.**

____________________ External Examiner	__________________ Signature	________________ Date
____________________ Internal Examiner	__________________ Signature	________________ Date
____________________ Chairperson	__________________ Signature	________________ Date
____________________ Department Head	__________________ Signature	________________ Date
____________________ School Dean	__________________ Signature	________________ Date
____________________ Post Graduate Dean	__________________ Signature	________________ Date

Declaration

I, Mati Oljira Regassa, declare this M.Sc. thesis is my original work and has not been presented for the fulfillment of a degree in this or any other university, and all sources and materials used for the thesis have been acknowledged.

Signature: ______________________Date: __________________________

Certification

The undersigned certify that he has read and here by recommend for the acceptance by the Adama Science and Technology University a thesis entitled: **Design and Modeling of off-grid DC Micro-grid for DC Homes: Case Study of Lake Ziway Highland (Tullu Gudo Island)** in partial fulfillment of the requirements for the degree of Masters of Science in Electrical Power Engineering.

Getachew Biru (Dr.-Ing)	________________	__________________
Advisor	Signature	Date

Acknowledgment

I would like to begin by thanking my advisor, **Dr.-Ing Getachew Biru**. I am grateful for his assistance and guidance throughout the graduate program. I would also like to thank rest of my graduate committee. Foremost, I would like to express my deepest gratitude to my family; especially to my Father **Oljira Regassa**. My father was a person, I looked up too and could always count on when things weren't going so well. Without his love and support none of this would have been possible. Mr. Ibsa Kumera(MSc) provided emotional and technical support that can never be repaid. In addition, I would like to say thanks to my friends for their support, and making college a great experience.

Abstract

This thesis presents a design and modeling of off-grid DC micro-grid for DC homes: case study of Ziway lake highland (Tullu Gudo island). The renewable energy sources, such as solar photovoltaic, wind, and other alternate source have huge potential to solve the problem of energy in the rural area of Ethiopia. To provide an economical and sustainable power to rural areas renewable energy systems are very much suitable. The primary goal of this thesis is to design, model and control an energy efficient, sustainable and less expensive off-grid DC micro-grid to promote microgrid application for rural electrification in Ethiopia, and to manage local electricity generation and storage systems. This DC micro-grid has an appropriate bus voltage of DC to supply efficiently a home load. A home load may include the appliances of lighting, TV, mobile charger, tape recorder/radio, refrigerator, and some cooking appliance. MATLAB is used to model and control an off-grid PV source, energy storage system, and distribution network for five (5) DC homes. In this study, design, control and modeling of each component has been accomplished. The validity of the off-grid DC micro-grid is evaluated by using simulations in Simulink software. Compared to the AC model, the power loss is reduced by close to 43% in the DC model, when factoring in standby loss. If standby loss was eliminated from the AC model, DC distribution would still reduce the power loss by almost 21%. The study shows that a 48V off-grid DC micro-grid is effective solution versus the existing AC system. Cost analysis also shows the feasibility of the proposed system as compared to commonly used AC distribution network.

Keywords: DC micro-grid, Energy storage, DC loads, AC system, photovoltaic panel and simulation

Table of Contents

List of Figures

List of Tables

List of Abbreviations

AC	Alternative Current
DBS	Direct Current Bus Signaling
DC	Direct Current
DER	Distributed Energy Resources
ES	Energy Storage
ESS	Energy Storage System
IGBTs	Insulated Gate Bipolar Transistors
LA	Lead Acid
LED	Light Emitting Diode
LVDC	Low Voltage Direct Current
MATLAB	Matrix Laboratory
MG	Micro Grid
MPP	Maximum Power Point
MPPT	Maximum Power Point Tracking
NASA	National Aeronautics and Space Administration
NMA	National Metrological Agency
PFC	Power Factor Correction
PSCAD	Power System Computer Aided Design
PV	Photovoltaic
SOC	State of Charge
TV	Television

Chapter 1

Introduction

1.1 Background

Roughly 1.1 billion people in developing countries in rural areas (about 381 million in Africa, 60.08 million in Ethiopia), are living without access to reliable electricity. People in these areas live in poor living environments and are disconnected with the rest of modern digitalized world. So, the use of electricity is becoming an essential part of life [1],[2].

The paper [6] describes that grid extension does not guarantee access to electricity for rural customers, especially for the case of long distance between the load center and the national electrical grid, and other reasons. One solution to the problem of long distances is to use locally available renewable energy sources, such as hydro-plants, solar PV, biomass or wind power generators, and thereby create a local distribution network for the area, which connect a number of villages.

The use of renewable energy in the world grew by an unprecedented manner and the cost of generating local power generated from solar PV is decreasing daily [7]. So, the distributed energy resources (DER) are emerged as a promising option to meet the growing customer needs for electric power with an emphasis on reliability and power quality.

AC and DC micro-grids are very good elements for the integration of renewable and distributed energy resources. Many studies have been conducted on the AC micro-grid but not on the DC micro-grid. Therefore, there is a need to study and evaluate the benefit and costs of DC micro-grid to implement it on a wider scale [8].

Today, with the majority of electronics and appliances being used in the household using DC voltage, DC distribution is being studied as a viable alternative to AC. DC distribution also benefits renewable energy generation that generate DC power, such as photovoltaic(PV), by reducing the number of energy conversion steps. In an AC power system including AC micro grids, DC power from photovoltaic (PV) panels or fuel cell generators has to be converted into AC using DC/AC inverters before the connection. In order to supply DC loads, AC power has to be converted to DC. The embedded AC/DC and DC/DC converters are required for various home and office facilities to supply different operating DC voltages. Even for some conventional equipment driven by AC motors such as refrigerator and air conditioners require DC voltage due to advanced control techniques used for energy efficiency. DC grids are increasing recently due to the development and deployment of renewable DC power sources and their inherent advantage for DC loads in commercial, industrial and residential applications [9].

DC microgrids are an effective means of achieving the efficiencygains needed to make rural microgrids cost-effective. The DC bus is the simplest and common interconnection bus. This system has no frequency and phase control requirements, and it needs fewer power converters (unlike DC-AC-DC conversion), high efficiency and high reliability compared to the AC interconnection bus [[10], [11], [12]. There is no need of frequency, phase, or reactive power control. Power qualityis not affected by inrush current, single-phase loads and single-phase generators. Stability control tends to be simpler in DC systems. By using an appropriate DC voltage to supply electronic loads, the rectifier and the PFC circuit can be removed from the loads [12].

Studies suggest that cost-reduction is possible through gains associated with improved power- conversion efficiencies that can be realized with a fully DC microgrid [1]. So, the primary goal of this study is to design an energy efficient DC micro-grid to promote microgrid application for rural electrification in Ethiopia, and to manage local electricity generation and storage systems.

1.2. Motivation

The off-grid DC micro grid project is a solution to challenges of rural electrification. It will provide self-sustaining DC power through various forms of renewable energy such as photovoltaic, hydropower, wind, and human-powered generation. The DC micro-grid is used to provide the most basic living necessities such as room lighting, electric stove for cooking, TV, mobile charger, tape recorder/radio and refrigeration. This renewable form of off-grid DC micro-grid energy will replace the currently used liquid fuel, gas, biomass or animal waste, to sustain the daily energy necessities of Ziway Lake Island (Tullu Gudo Island), Ethiopia.

1.3 Statement of the Problem

Ethiopia is one of developing countries with much of the population lives in remote or rural areas, most of these are not yet electrified, and they rely on fossil fuels (mainly kerosene) for their primary lighting needs, dung and wood for cooking. Statistical data of Ethiopia shows that [13], rural population percentage is decreasing by 19% from 1990 to 2016, because of youth immigration to urban. If this study makes rural areas comfortable for living, this thesis simply stops this migration and attract investors to work in rural areas where raw material cheap labor cost is available. One of the ways to change these people living standard is by supplying affordable and reliable energy.

Electrifying these remote areas by extending grid system to these rural communities is difficult and needs high connection costs because of they are characterized by either low-density settlement with relatively large distances between households, or villages with fewer inhabitants. This has hindered the use of modern sources of energy.

The renewable energy sources, such as solar photovoltaic, wind, and other alternate source can solve the problem of energy in the rural area such as provide power for irrigation, improve medicine cold storage in health centers, mitigate health problems related with indoor air pollution in using kerosene for lighting and wood for cooking, help women tasked with collecting wood and animal manure in saving their time and energy, for night education for day time workers, etc.

Most of the equipment (motor loads, pumps, lighting, information technology equipment, battery charger, etc.) uses DC rather than AC; all of these systems require the conversion of power from AC to DC for their operation. Having directly available DC power can increase energy efficiency by eliminating losses associated with DC-AC-DC conversion, as well as increase reliability due to the elimination of several transformer components. Batteries, capacitors, and so on can be used to store DC electricity. The use of AC in place of DC increases the cost of storage devices, because of using AC to DC conversion and related.

Thus, in this thesis an off-grid DC micro grid renewable power generation system integrating this vast solar resource is designed, modeled and controlled to electrify the community living in Ziway lake highland (Tullu Gudo Island), which is found in Oromia regional state, Ethiopia.

1.4. Objective of the Study

1.4.1. General Objective

The general objective of this thesis work is to design off-grid DC micro-grid and then make a comparative analysis of the DC micro-grid with the currently existing AC system.

1.4.2 Specific Objectives

The following specific objectives are formulated to accomplish the general objective of the study

- Identify one particular rural village (Tullu Gudo Island) in Ethiopia and make an assessment of the energy resource and power requirement.
- Evaluate the benefits of using DC instead of AC.
- Select appropriate voltage for the supply system and design a reliable and efficient power generation system.
- Design distribution system from the DC micro grid to individual homes and design the control system of the off-grid DC micro grid.
- Evaluate the design and cost benefits of DC vs. AC distribution system.
- Simulate the system using MATLAB software and evaluate performance benefits of the off-grid DC MG energy system.
- Draw relevant conclusion and future work for practical implementation of the system.

1.5. Scope of the Study

The scope of the study includes:

- Design DC micro-grid energy system with the storage devices and build its mathematical model.
- Study the benefits of using DC load from the perspective of home loads.
- Design master slave control method for off grid DC micro-grid energy system
- Investigate the conversion system involved in off grid DC micro-grid energy system and the control system.
- Evaluate appropriate control strategy for the proposed off grid DC micro-grid energy system regarding to different operations.

1.6. Significant of the Study

- The study has great significance for the people living without electrical power, to get reliable and clear energy for household needs like mobile charging, lighting, TV, refrigeration etc.
- The study will benefit the governmental and nongovernmental organizations working on rural development to electrify remote villages in affordable way. This study will be initiator to investors to invest in micro-grid market in remote areas in Ethiopia.

1.7 Methodology

To successfully complete the thesis the following activities are conducted based on the order given.

a. Literature Review

An extensive literature review is conducted on the research area. Literary review on off grid DC MG energy system was performed to better understand the impact and benefits of the system.

b. Design and Modeling

In this section a design and modeling of off gird DC MG system is established to further study its performances. Modeling and Design of each element in DC microgrid, including the load demand is investigated and created. The system design and model are analyzed, in terms of its technical application, economic benefits, performances (losses, efficiency, quality and reliability and others). The control system of the DC micro-grid is studied and modelled as well using MATLAB.

c. Simulation

With the design, modelling and control method at hand, various simulations of the off-grid DC MG energy system are conducted to analyze and test the system, and correct any errors, and evaluated the system in terms of efficiency, stability, applicability and environmental aspects. Software like MATLAB/SIMULINK or PSCAD are used as required.

Chapter 2

Theoretical Background and Literature Review

2.1 Theoretical Background

2.1.1 AC Distribution

Early 20th century, power systems were developed as isolated networks looking after local needs. But as the demand for electric power and transmission distances grew, voltages had to be raised to maintain efficiency, and networks required interconnection for reliability. DC systems were constrained due to the complexity of motor and generator design and non-availability of equipment for voltage transformation. Tesla's invention of the induction motor simplified the design of machines for the majority of industrial applications. This led to the dominance of alternating current (AC) over DC for generation, transmission, and to a large extent the utilization of power. This invention cemented the way for the AC infrastructure to build over the past century [29].

2.1.1.1 AC Distribution Infrastructure

The grid "topology" used in an electrical energy distribution can vary according to practical constraints of budget, requirements for system reliability, and the load and generation characteristics. Figure 2.1 shows a typical power generation and distribution system used around the world [33]. The power generation sources comprise fossil fuels, nuclear, hydro, and renewables. Step-up transformers are used to step up the transmission grid voltage in hundreds of kilovolts in order to transmit power over long distances with minimum losses. The resistive power losses in electric transmission lines are directly related to the amount of current flowing through the conductor($P_{Loss} = I^2R$) once in the close proximity of the load, the voltage is stepped down and distributed at voltages required by the load (in Ethiopia, domestic loads are supplied with 220Vac at 50 Hz).

The infrastructure needed for this classic generation, transmission, and distribution requires high initial investment. Along with high initial costs, the AC system is also very complex and has many disadvantages in power distribution when compared to a DC system.

Figure 2.1: Transmission and distribution grid structure within the power industry [33]

2.1.1.2 Disadvantages of AC distribution

One of the many disadvantages of an AC transmission line is its limited capacity in transmitting power. The effective voltage of a conductor in an AC system is limited to 70.7% of the peak value. A like conductor in DC transmission can transmit approximately 30% more power because the peak and RMS values in DC are same.

Also, the current density of alternating electric current is non-uniform and more current flows near the surface of the conductor than the core, known as the “Skin Effect”. This condition decreases the amount of power that could be transmitted through a conductor because the middle portion of the conductor is not being used.

As shown in Figure 2.2, the current density for a DC conductor is uniform throughout, which is not true in AC conductor [33]. In an AC conductor, skin depth decreases as the frequency of current increases, thus current only flows mainly near the surface of the conductor [33].

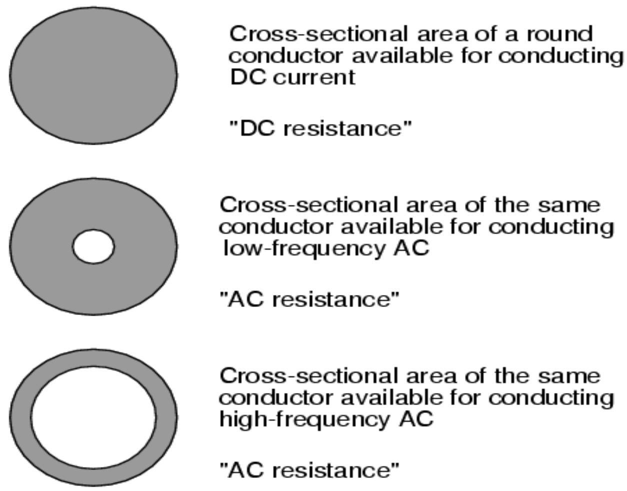

Figure 2.2: Skin depth decreases with increasing frequency [33]

The power factor of the AC system is another variable that affects AC power transmission. The reactance of AC transmission lines lowers its power factor which leads to reactive power being drawn out of the generator, and subsequently less real power is delivered to the load. Another issue of an AC system is its frequency, which is required to be at 50 Hz for a stable system. An inaccurate frequency control does not allow efficient flow of power from multiple generators into the grid network. Another phenomenon in AC transmission is the corona discharge effect in which electrical breakdown is caused by ionization of surrounding air of conductors at voltage amounts greater than that of the critical breakdown voltage [34]. Many of the domestic loads such as home appliance, electronics, and entertainment systems require DC power for their operation. The incoming AC from the power outlet has to be converted to DC in order for these loads to work. This AC to DC power conversion introduces power losses into the system. Figure 2.3 shows the conversion stages which are required in an AC system for the DC loads [35]. Additionally, in case of renewable sources, which (generate DC power), the current AC system requires two conversion stages before power could be delivered to the load.

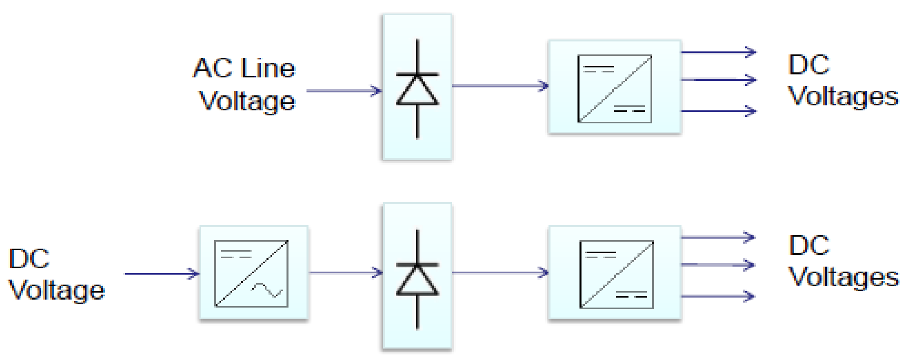

Figure 2.3: Conversion stages in an AC system [35]

A DC distribution system would eliminate the AC to DC conversion by more efficient DC-DC conversions. Another benefit of a DC system is that it is less costly since components are rated at lower voltages. Largely the DC distribution system is less complex, more efficient and consumes less space. However, AC system was preferred over DC system for the past century because DC did not have the capability to step-up or step-down voltage without the power electronic technologies. The power electronic industry has since developed highly reliable and well-performing technologies capable of these tasks, and DC distribution is now considered as an optimal solution to improve distribution efficiency.

2.1.2 DC Distribution

The idea of incorporating one or multiple renewable energy sources to support the DC system is unique. DC system depicts lack of frequency stability, reactive power issues, skin effect, and conversion losses compared to AC power system. Using direct current to distribute power is not a new concept. As mentioned earlier, Edison was promoting DC distribution network during the "War of Currents" era in 1890's. So, several potential benefits are driving new interest in DC power delivery systems in the 21st century. Also, RV, Telco and Data centers, aircraft, spacecraft, and ship already used DC distribution [36].

2.1.2.1 Recreational Vehicle(RV) DC Distribution

First example of an existing small DC power distribution system in use is an RV's electrical system, as illustrated in figure 2.4 [37]. The RV's motor drives an alternator that produces AC voltage, which is rectified to 12-volt DC to charge the on-board batteries and supply power to the DC appliances. This 12-volt DC distribution has its own fuses, receptacle, and wiring. This system provides for the key components of an RV, such as light, water, heat, fans and motor, refrigeration, entertainment, and safety [37].

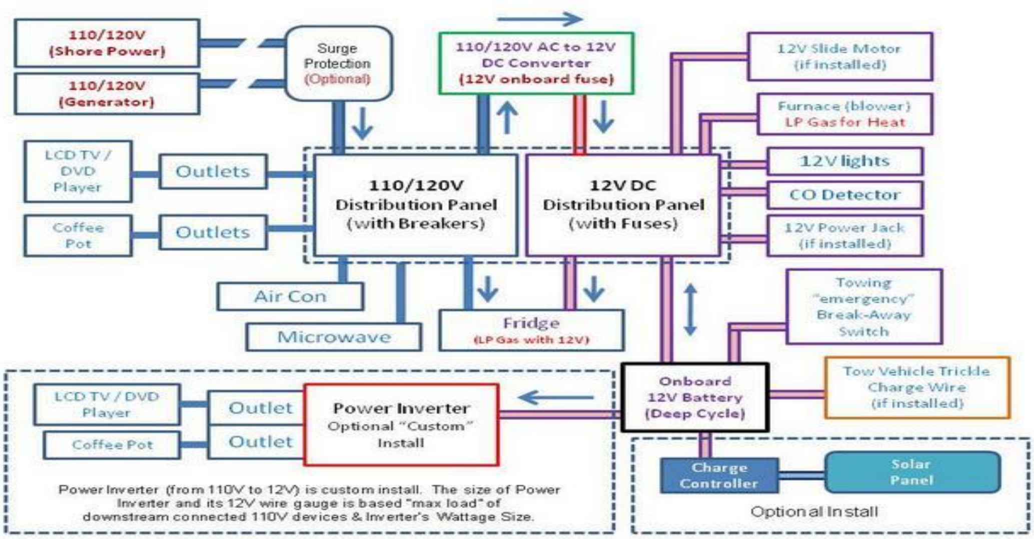

Figure 2.4: 110/120V – 30 Amp RV wiring configurations [37]

As showed in Figure 2.4, there are cases when solar panels are also used to power the DC appliances and charge the batteries. In these cases, a charge regulator controls the power flow to the battery in order to protect from overcharging. Importantly, the DC system differentiates itself at this point because it is not necessary for the RV motor to be on as the basic appliances are running. This can be helpful in instances such as when the family is camping. Another application of a DC distribution system at a larger scale is in Telco and Data Centers (and it is discussed as below).

2.1.2.2 400V DC Distribution in Telco and Data Centers

Telco and data centers around the world are major consumers of power. In a typical 480 VAC data center (Figure 2.5), less than half of the power is delivered to the actual computer load, which includes microprocessors, memory and disk drives. The conventional power delivery architecture is burdened by many power conversion stages, as illustrated in Figure 2.5 [38]. Moreover, each conversion stage creates inefficiency which wastes energy, produces heat, and increases the load on the central part of cooling system of the firm.

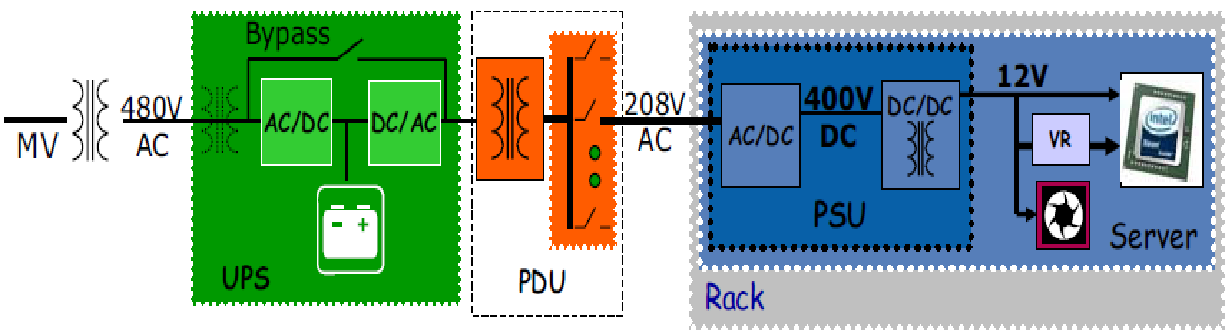

Figure 2.5: Conventional 480Vac distribution in the United States [38]

In [38], a 400 VDC distribution in Telco and Data center was evaluated to improve energy efficiency of the system. The findings of this study showed that system efficiency improved significantly in power delivery architectures when power conversion stages were eliminated by directly feeding 400 VDC (Figure 2.6) [38]. Figure 2.7 displays the efficiency plots of power distribution architectures studied in [38] for the Telco and Data Centers.

This study concluded that the two electrical architectures, 400 VDC and 48 VDC, yield the highest efficiency because the conversion stages are eliminated.

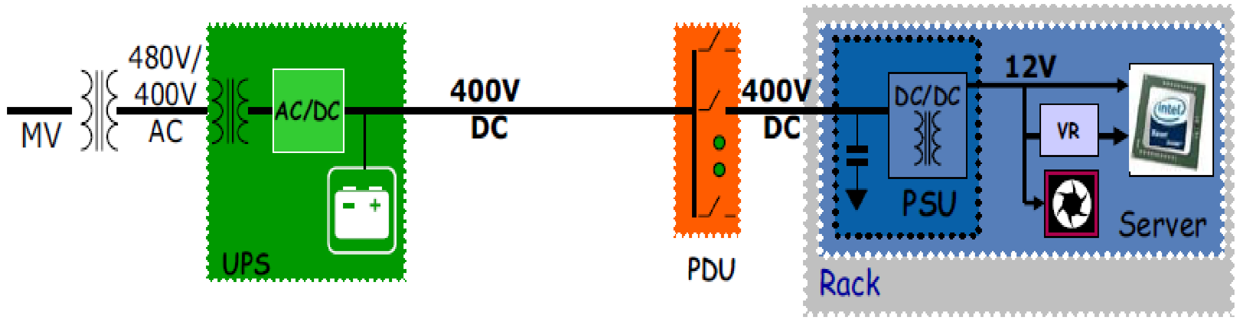

Figure 2.6: Proposed facility-level 400V DC power distribution [38]

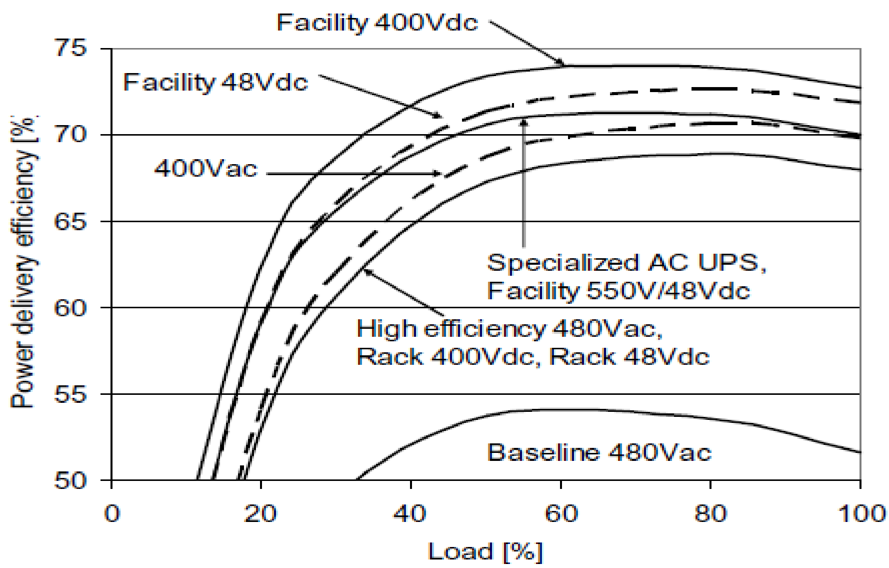

Figure 2.7: Comparison of calculated efficiencies as a function of load [38]

2.2 DC Voltage Level Selection

In the DC systems, voltage level is a vital criterion that can have effects on the safety and performance of the entire system. The authors in [39] investigated different voltage levels performance for 400Vdc, 325Vdc, 230Vdc, 120Vdc, and 48Vdc and considered the 48Vdc system the most applicable for residential DC systems and the 400Vdc for commercial facilities based on efficiency analysis.

In addition to that there is a variety of voltage levels in DC that can be used to be voltage level of LVDC. However, thorough study needs to be done to choose the amount of voltage level for LVDC. There are several studies that have examined the amount of voltage suitable for LVDC grid. Table 2.1 shows list of voltage levels recommended for LVDC based on prior researches and studies.

Table 2.1: List of voltage levels recommended for LVDC.

Authors	Voltage Levels recommended
Pellis [40]	< 120 V
Williamson [41]	24 V < V < 48 V
Li [42]	< 120 V
Anand [39], [43]	48 V

Based on Table 2.1, it can be concluded that there are variety voltage levels that has been recommended by several authors. Anand [39], [43] and Williamson [41] have recommended Voltage level 48 V to be implemented in LVDC micro-grid. Therefore, in this study, the median value between the recommendation voltage levels from Anand and Williamson that comply the IEC 60038 and BS7671:2008 standards which is 48 V is chosen. This is due to the need to choose suitable amount of voltage DC which is applicable to be used in DC micro-grid and also stepped down by using boost converters with PI controllers before it is connected with household appliances which is working on relatively low voltage.

2.3 Control Method of Off-grid DC Micro-grid

In this thesis, a “Master Class” control is proposed to balance the DC voltage bus and to control the power supply to meet the DC load demand in off-grid mode. In this control, one-unit source acts as a “Master” controlling the full system, while the rest of the units work as current sources (i.e. as “Slaves”). In this way, there will not be voltage difference between the outputs of the DC sources, because the master unit regulates the voltage values of all the output units, therefore it will not circulate current between the sources [44]. The DC bus voltage in the micro-grid is sensed and compared with the reference voltage chosen in the section 2.2 (48V), the error is processed through a compensator (PI block) to obtain the desired impedance current reference for the current loop. This compensator can be expressed in the following way:

$$I_{L_{REF}} = K_P(V_{REF} - V_{MG}) + K_i \int (V_{REF} - V_{MG})dt \quad (2.1)$$

The power flow is controlled by a current controller who compares the impedance current in the master unit with the reference current desired to stabilize the system, the error is processed through another PI block to obtain the desired duty cycle for the converter which acts as a master. The PI block can be expressed as:

$$d = K_P(I_L^* - I_L) + K_i^* \int (I_L^* - I_L)dt \quad (2.2)$$

In this study, the ESS is used to control the voltage level and the power flow through a bidirectional converter; the main objective of the bidirectional converter control is to maintain a constant DC-bus voltage as a reference value and discharge/charge current from/to the battery bank according to the required load power. Since, the micro-grid is working in off-grid mode, this source will act as a "master" remaining the voltage at 48V and meeting the DC load demand.

2.4 Distribution Network for DC Homes

This DC home network, a single or five (5) to ten (10) DC homes operates in islanding mode, as showed in Figure 2.8 [20]. This type of configuration is suitable for remote villages with widely disperse population and it can have one or multiple renewable sources generating DC power. Also, it allows the exchange of power in a small cluster of DC homes and suitable for more concentrated pockets of remote villages. In addition, this approach offers betters system reliability and lowers the cost of the study.

This thesis focuses on the design, modeling, control, simulation, and performance evaluation of this DC micro-grid distribution network, which is presented in greater detail in the following chapters.

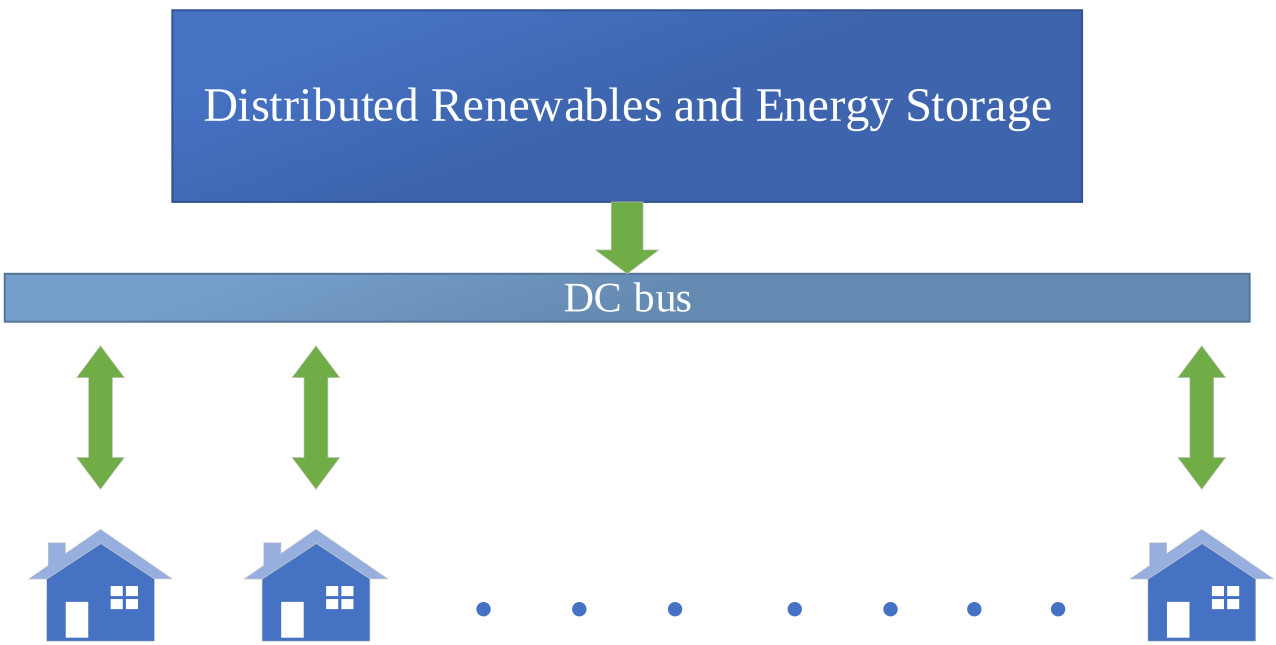

Figure 2.8: Distribution network for DC homes

2.5 Literature Review

Related Work

Over the past few years several researchers have been carried out on hybrid power systems, such as Author in [14], who recommended microgrid composed of two distributed generation sources (photovoltaic panels and biofuel generator), one energy storage device (battery bank), and both AC and DC loads, including a plug-in hybrid electric vehicle, is done. The microgrid is composed of a main DC bus and also an AC bus. AC bus is aimed to drain/inject power in utility grid. When several converters are connected to a main bus some problems like (variation in voltage, incorrect power/load sharing among converter) can arise in the system. In this paper which converter operates under distinct situations, their specifications and control methods in the residential MG is not studied.

Author [15] proposed AC-DC microgrid, dc and ac power sources supplying ac and dc loads. Ac buses supply power full devices like air conditioner, washing machine, etc. and dc buses supply lighting system, consumer electronics and provide charging electro mobile. And also, advantages of DC microgrid are discussed. But there are some gaps that need further investigation in the field of dc micro grid. Example, development of DC microgrid-distribution of DC current, Installation of DC distribution box in every house, etc. needs further explanation and study.

DC Micro-grid platform is designed for solar energy sources, and for practical applications such as lighting, cooking and computing in [16]. DC micro-grids can optimize the use of electronic devices, electrical storage, and distributed generation. According to Author in [16] those two (dc-ac-dc) conversions yield an approximate 10-40% power loss. The Power Server accepts both AC and DC as power inputs and then produces only DC power output. Author in [16], test the system in few number of test points, if this thesis increases test points, more number of sections can be checked thoroughly.

Author [10] presented power control strategies of DC Microgrid with variable generation and energy storage. Different with the centrally control method, the droop control based on the DC-bus signaling (DBS) is used in this paper. DC bus signaling (DBS) induce DC bus voltage level changes to realize the communications between different micro sources and storage interface converters, it can maximize the use of the renewable sources, and achieved optimal control of the DC microgrid.

Author [17] presented a design example of DC bus voltage regulator. The DC bus voltage regulators in this case are used to maintain DC bus voltage at constant value and therefore used as a point of common coupling of several available renewable energy sources. The results obtained from off-line simulations were used to determine suitable system parameters for best results, but the result is not included in this paper.

Several modelling studies on PV-wind turbine power system have been conducted. Among them, Kim [18] developed a grid-connected photovoltaic model using PSCAD for electromagnetic transient analysis where a simple circuit model of the solar array was used to easily simulate its inherent characteristics with the basic specification data. Tsai [19] implemented an insulation-oriented PV model using the MATLAB/Simulink software package. Taking the effect of sunlight irradiance on the cell temperature, the model took ambient temperature as reference input and used the solar insolation as a unique varying parameter. The output current and power characteristics were simulated and analyzed using the proposed PV model. The model verification was finally confirmed through an experimental measurement.

To allow the PV system to produce the maximum possible power, significant number of maximum power tracking techniques and algorithms have been developed. Femia [20] and Tariq [21] suggested the most widely used method known as the Perturbation and Observation method. In their paper, a microcontroller-based maximum power point tracking (MPPT) was realized. Two tracking algorithms, namely, Perturbation and Observation algorithm and maximum power point voltage (MPP) algorithm were implemented. The MPPT was tested under varying insolation and load conditions. It was shown that with the Perturbation and Observation algorithm, the controller took a relatively moderate time to track the maximum power point.

The DC-DC power electronic interfaces of batteries used in microgrid was proposed and studied by Sofla [22]. The study was conducted to investigate how the stability of the islanded microgrid depends on its response speed to the transients. The paper focused on inner and power controllers of the DC-DC bidirectional converters for interfacing batteries in microgrid. The inner control techniques were discussed and a control strategy for the operation of batteries in different modes was proposed. Wei [23] proposed a parallel structure of bidirectional buck/boost converters and a power-tracking control scheme for wind energy storage system applications. The converter performance was studied and compared to single-unit topologies. The proposed converter was found to have smooth currents and fast dynamics which allowed a reduction in the converter switching frequency and DC filtering capacitor.

Ramprabhakar [24] gave a paper which described a control approach applied to dual bidirectional Voltage source converter for composite wind-solar-hydro power systems in order for these systems to operate in grid-connected and islanded modes. A control technique was devised based on sum of-product of load and utility voltages, which generated requisite phase angle for utility synchronization. The effectiveness of the control technique was demonstrated through simulation of the proposed scheme under constant as well as changing meteorological and load conditions.

Author [25] presented a performance study of a DC micro- grid when it is used a voltage droop technique to regulate the grid voltage and to control the load sharing between different sources. Some aspects about centralized (master-slave) and decentralized (voltage droop) control strategies as well as the procedures to design the controllers, with droop control, are presented and discussed.

In this thesis, a detailed design, model, control and simulation of a solar off-grid DC micro grid power generation system for DC homes with battery storage as a master control is proposed. Modelling and simulation are carried out using the MATLAB/Simulink software package, specifically SimPowerSystems, to verify the effectiveness of the proposed system. SimPowerSystems enables engineers to use model based designs to model and simulate electrical circuits and power systems within Simulink, and includes a comprehensive applications library which makes the interfacing of all the components of the solar-battery system a straightforward process for the user.

Chapter 3

Design, Modelling and Control of DC Micro-grid

3.1 Site Description and Solar Energy Data of Study Area

3.1.1 Site Description

Lake Ziway is one of the freshwater Rift Valley lakes of Ethiopia and located at 8°00′N 38°50′E.

Figure 3.1: Lake Ziway

It is located about 100 miles south Addis Ababa [26], on the border between the regions (or kililoch) of Oromia and of the Southern Nations, Nationalities, and Peoples; the woredas holding the lake's shoreline are Adami Tullu and Jido Kombolcha, Dugda Bora, and Ziway Dugda. The town of Ziway lies on the lake's western shore. The lake is fed primarily by two rivers, the Meki from the west and the Katar from the east, and is drained by the Bulbar which empties into Lake Abijatta. The lake's catchment has an area of 7025 square kilometers [27].

Lake Zway is 31 kilometers long and 20 km wide, with a surface area of 440 square kilometers. It has a maximum depth of 9 meters and is at an elevation of 1,636 meters [28] [29]. According to the Statistical Abstract of Ethiopia for 1967/68, Lake Zway is 25 kilometers long and 20 km wide, with a surface area of 434 square kilometers. It has a maximum depth of 4 meters and is at an elevation of 1,846 meters [30]. It contains five islands, including Debre Sina, Galila, Bird Island and Tulu Gudo, which is home to a monastery said to have housed the Ark of the Covenant around the ninth century.

The lake is known for its population of birds and hippopotamuses. Lake Zway supports a fishing industry; according to the Ethiopian Department of Fisheries and Aquaculture, 2,454 tonnes of fish are landed each year, which the department estimates is 83% of its sustainable amount. [32]. The shores and islands of Lake Zway are the home of the Zay people. In Ziway lake highland, Ethiopia. Tulu Gudo Island (shown in Figure 3.2) is approximately 11.185 miles off the southeastern coast of south Ziway, Ethiopia in the state of Oromia. It is an island and it has around 900 Zay peoples. On this island, there is no installed energy system.

Figure 3.2: Tulu Gudo Island

Geographically, Tulu Gudo Island or Tsion is a hot and humid island. It is a sunny island the equatorial belt. Thus, a completely clear or cloudless sky is common on this rift valley island.

3.1.2 Solar Energy and Surface Metrological Data of Tullu Gudo Island

The following solar **e**nergy and surface metrological data, and average monthly solar irradiation of Tulu Gudo highland have been collected and used for the design and modelling of off-grid DC micro-grid for DC homes.

Tullu Gudo Highland Solar Energy and Surface Metrological Data

Tulu Gudo Island receives 5.5 solar hours daily on average. The solar data and average monthly solar irradiation of this island have been collected from NASA and NMA as shown in the next Figures 3.3 to 3.4.

Variable	Jan	Feb	Mar	Apr	May	Jun	Jul	Aug	Sep	Oct	Nov	Dec
Insolation, kWh/m²/day	5.65	6.04	6.08	5.78	5.74	5.18	4.54	4.77	5.39	5.87	6.12	5.82
Clearness, 0 – 1	0.62	0.62	0.59	0.56	0.56	0.52	0.45	0.47	0.53	0.59	0.66	0.65
Temperature, °C	18.42	19.60	20.44	19.57	18.23	16.78	15.73	15.76	16.33	16.58	17.07	17.50
Wind speed, m/s	4.49	4.06	3.84	3.93	3.72	3.67	3.19	2.96	3.05	3.66	4.20	4.47
Precipitation, mm	27	43	78	112	135	98	128	136	140	88	35	16
Wet days, d	3.3	4.3	6.1	11.0	10.8	10.3	9.2	10.8	9.4	7.2	5.4	3.5

Figure 3.3: Ziway, Ethiopia - Solar energy and surface meteorology [30]

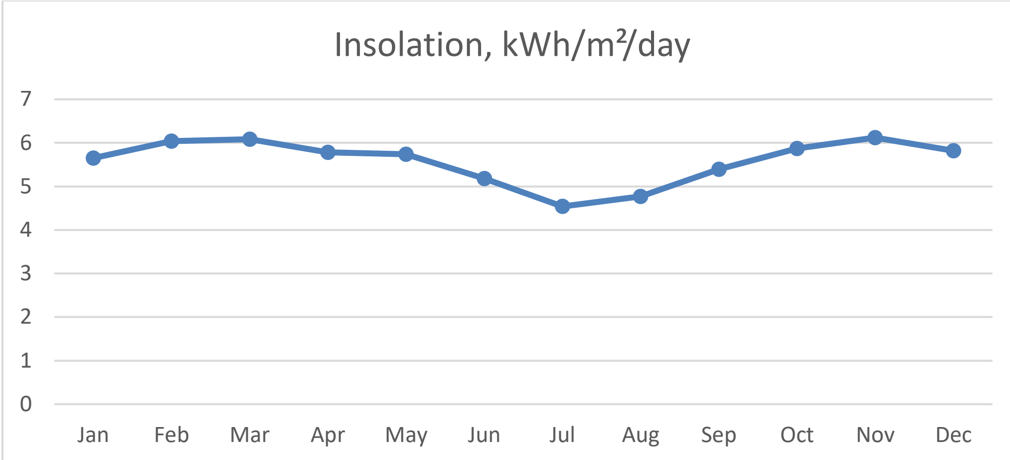

Figure 3.4: Average monthly solar irradiation of Tulu Gudo island

3.2 Load Selection and Energy Demand Estimation of Tullu Gudo Island.

The load has been selected from a publication by the Department of Energy [45] and contains average items that can possibly be found in rural village DC homes. As can be seen in Table 3.1 the DC load consumption is relatively low in islanding areas. For load flow calculations, the household appliances are modeled as loads which draw constant current from the DC distribution network.

3.2.1 Load Selection for Tullu Gudo Island DC Homes

In order to select the loads needed for the DC house it is important to consider the needs of the people living in Tullu Gudo island and the humanitarian goals of the DC house project and weigh them against the constraints that an isolated generation system provides. So, the selection strategy is first a set of basic home needs is defined, and loads are chosen to fulfill those basic needs. Then, if these "basic needs" loads do not fulfill the 500 W limitation, additional convenience loads are added. The basic humanitarian goals that should be met by the DC house are: lighting, some means of cooking, food storage, laptop charging and tape/radio as shown in Table 3.1.

Table 3.1: 12V and 24V appliances for low-power consumption [35]

Static load	Average power	Average voltage	Average current	Units	Time per day per units (hours)
LED lighting	13 W – 24 W	12 V, 24 V	20 mA – 550 mA	3	8
DC fans	6 W – 72 W	12 V, 24 V	0.5 A – 3 A	1	1
Radio	2AA Batteries	3 V – 5 V	-	1	5
DC hot plate	78 W	12 V	-		4
Computer	-	19 V	3.5 A – 4 A		1
Mobile/laptop charger	30 W	12 V	2.5 A	2	6
Refrigerator	12 W	12 V, 24 V	0.5 A – 1 A	1	24
TV	56 W	12 V, 24 V	1	1	6

But, for the case of cooking device a conventional electric powered oven and electric powered stove top also present problems in their wattage ratings. The typical conventional oven requires 220 V, and will typically draw 3 Amps of current, yielding an unusable wattage rating of 720 Watts. The best alternative to cook foods at a low wattage proved to be a device that is characterized by its long cook times and relatively small wattage requirements. The crockpot cooking device fulfilled this role perfectly. A crockpot or slow cooker is a device that operates at low wattage for extended periods of time (usually 8 hours) to cook food. This power profile fits well with the DC house constraints. The model examined as a candidate is the 12 Volt RoadPro Slow Cooker Crock Pot. The device is rated at 78 Watts [20], well within acceptable levels for the DC homes study.

In general, Tullu Gudo island has around 900 Zay peoples and the houses are widely dispersed. But, on some areas around five to ten houses are located near to each other. Each DC house in the village needs 500 W peak power and the number of homes considered are approximately five (5). Thus, at peak time the total power supplied to the cluster of villages is 2.5KW, neglecting losses in the energy and delivery system. The design requirement is thus for a 1 PV system delivering 24V Vdc. The minimum DC voltage to be supplied to the DC Bus is 48 Vdc from the three standard DC bus voltages and which is the most applicable for residential DC systems. Therefore, for the selected loads for the study area, a 2.5KW Solar system with energy storage device is to be designed, modeled and controlled for the continuous and efficient utilization of energies in the following sections.

3.3 System Design, Modelling and Control

The system discussed in this thesis is a 2.5 kW off-grid DC micro grid system for DC loads. Consists of a DC generator, energy storage, DC loads and a power electronic interface to off-grid DC micro grid energy system. The proposed off-grid DC micro-grid system supplies power lighting, some means of cooking, food storage, laptop charging and tape/FM radio for the villagers. The supply side of the off-grid DC micro grid energy system includes a 2.5 KWp PV array, using 56 different types of modules with seven in series and six modules connected in parallel and energy storage. The distribution system is DC supplying DC loads. After a detailed explanation about the unit models, the control of DC micro-grid energy system is analyzed by highlighting how the power electronic systems are designed and controlled to achieve their goals. The main renewable energy is PV and ES that are controlled through DC-DC converters. Particularly, the photovoltaic arrays by a boost converter, the energy storages by a bidirectional chopper. As stipulated in the introduction, multiple renewable sources can be used to generate power for the DC house as well as the system is intended to power rural households it must be cost effective; therefore, only solar energy system is retained. Therefore, this thesis only focuses on solar power generation as the source of power for the off-grid DC micro grid for DC homes. Figure 3.5 shows the fundamental block diagram of the proposed design and control for off-grid DC micro-grid distribution network.

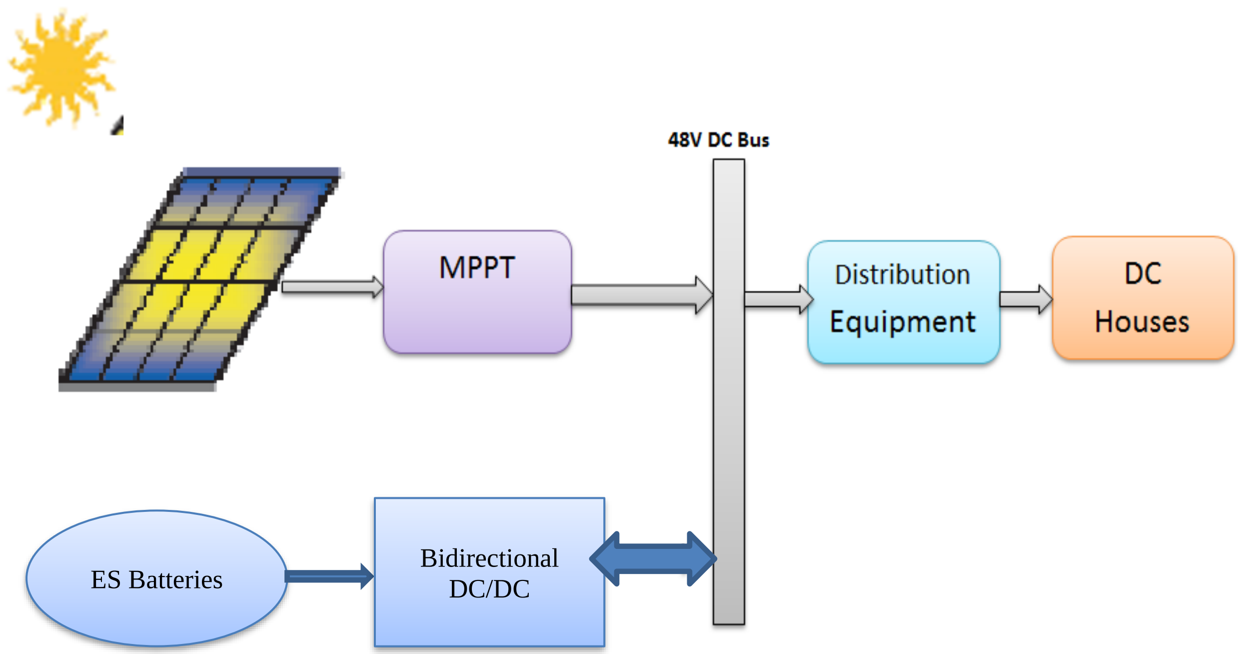

Figure 3.5: Block diagram of the proposed off-grid DC micro-grid

3.3.1 Photovoltaic Design, Modelling and Control

Photovoltaic Cells

Photovoltaic cell are devices that transform the sun irradiance into DC current, the common types of PV Cells produced are:

- Monocrystalline Silicon Cells
- Multicrystalline Silicon Cells
- Thin film Silicon
- Amorphous Silicon

In Figure 3.6 a simplified equivalent circuit model of the PV is presented. The output current of a PV module can be obtained from the below equation 3.1,

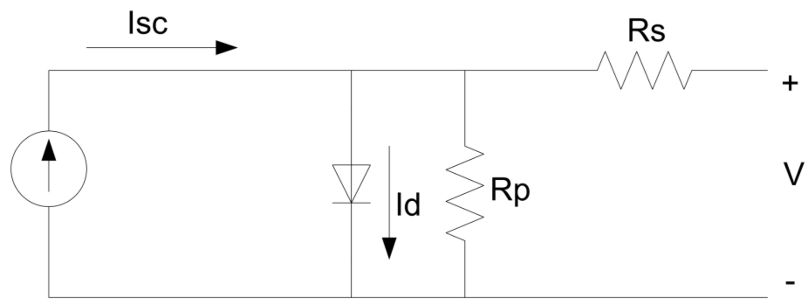

Figure 3.6: Equivalent circuit model for a PV [47]

$$I = I_{SC} - I_D - I_{RP} = I_{SC} - I_0\left[e^{q\frac{V+IR_S}{nV_T}} - 1\right] - \frac{V+IR_S}{R_P} \tag{3.1}$$

Where :

I_{SC} = Cell short-circuit current at 25℃ (°C)

I_D = Diode's saturation current (A)

I_0 = Is the reverse saturation current of the diode

V_T = Thermal voltage of the diode

q = 1.6022×10^{-19}, electric charge, (C)

n = Diode's quality factor

The effect of parallel resistance (Rp) is very small in a single module because its value is close to ∞, therefore it doesn't affect the PV current value. Usually a PV array consists of a group of PV modules for obtaining high power. Those modules in a PV array are connected in series-parallel combinations [11]. The output current, if Rp is considered ∞, of a PV array can be obtained from equation:

$$I = N_P I_{SC} - N_P I_P = N_P I_{SC} - N_P I_0\left[e^{q\frac{V+IR_S}{nN_S V_T}} - 1\right] \tag{3.2}$$

where N_P and N_S are the number of cell in parallel and in series respectively.

The current versus voltage and power versus voltage characteristics of a PV array are similar as the characteristics of a single module shown in Figure 3.7.

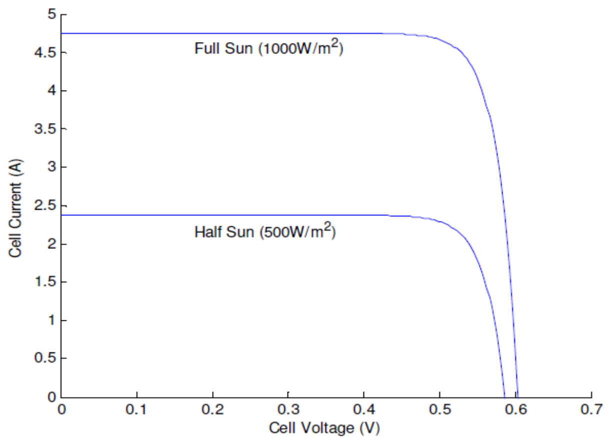

Figure 3.7: I-V characteristics of PV

3.3.1.1 Photovoltaic Model

For the PV array, the SX190W 's model from BP Solar manufacturer has been chosen. The parameters are shown in next Table 3.2:

Table 3.2: PV data sheet

Maximum Power (Pmax)	190W
Voltage at Pmax (Vmppt)	24.3V
Current at Pmax (Imppt)	7.82A
Short-circuit current (Isc)	8.5A
Open-circuit voltage (Voc)	30.6V
Temperature coefficient of Isc	(0.065±0.015) %/ºC
Temperature coefficient of Voc	-(111±10) mV/ºC
Temperature coefficient of power	-(0.5±0.05) %/ºC
NOCT (Air 20ºC; Sun 0.8kW/m^2; wind 1m/s)	47±2ºC

3.3.1.2 PV Panel Sizing Calculation for the Study Area

At this stage, the study shall calculate the number of modules that are needed to supply a load of 2.5kW in the Island of Tullu Gudo, Ethiopia. To meet the load demand selected in section 3.2, the renewable energy source (PV-arrays) with the storage devices must be sized properly so that efficient power utilization can be achieved. Additionally, the adequate sizing of PV array is also important to prolong the life of the system components, house appliances, and battery bank. PV array sizing is based on the lowest insolation month (critical month) of the study area. From the data in Figure 3.4, it is clear that the lowest insolation month in Tullu Gudo island is July when the average insolation is $4.54\frac{\mathrm{Kwh}}{\mathrm{m}^2}$.

The design is done using the worst-case insolation levels of $4.54\frac{\mathrm{Kwh}}{\mathrm{m}^2}$. The total daily energy demand for the system is based on 4 hours at full load, 12 hours at 60% of the load and 8 hours at 30% of load (night). Total energy demand for a 2.5kWp system is calculated using:

$$\text{Energy demand / day} = 2.5\text{Kw} \times 4\text{hrs} + 1.5\text{Kw} \times 12\text{hrs} + 0.75\text{Kw} \times 8\text{hrs} = 34\text{kwh}$$

BP Solar SX3190W solar module is selected for the system due to its competitive price per watt which produces 190W at 1kW/m² and 25ºC at STC (Appendix B). Using the formulas (3.1) to (3.2), this study can compute the power generated by the photovoltaic module. These energy demand calculations take into consideration the energy required to charge the battery bank. Table 3.3 shows the PV array sizing based on 85% system efficiency.

Table 3.3: PV Modules and Array Sizing

PV_ sizing_ insolation _4.54W/m^2

	2.5KW system
	Max eff
C1 Total energy demand per day (Wh)	34000
C2 System efficiency	0.85
C3 Required array output per day (Wh) (C1/C2)	40,000
C4 Selected PV module max power voltage(V) at STC (0.85)	24
C5 Selected PV module guaranteed power output(W) at STC	190
C6 Peek sum hours at design tilt for design month	4.54
C7 Energy output per module per day(Wh) (C5*C6)	817.2
C8 Module energy output per module per day(Wh) (DF*C7)	
DF = 0.80 for hot climates and critical applications.	
DF = 0.90 for moderate climates and non-critical applications	735.48
C9 Number of modules required to meet energy requirements (C3/C8)	56
C10 Number of modules required per string (A2/C4)	2
C11 Number of strings in parallel (C9/C10) rounded	27.5≈28
C12 Total Number of modules (C10*C11)	56

The PV model considering in this study is composed by 28 parallel strings, each one devised by 2 modules connected in series, for an overall nominal power of 2.5kW.

3.3.1.3 Control of PV System

DC/DC Boost Converter

The PV unit considered in this study gives an output voltage value lower than the required DC micro-grid. Therefore, the voltage level has to be increased and the converter has to work in the boost mode. Figure 3.8 shows the schematic of the boost converter with a power flow from left to right, the main components are the inductor L, the output capacitor C, the switch IGBT, the diode, and the load R.

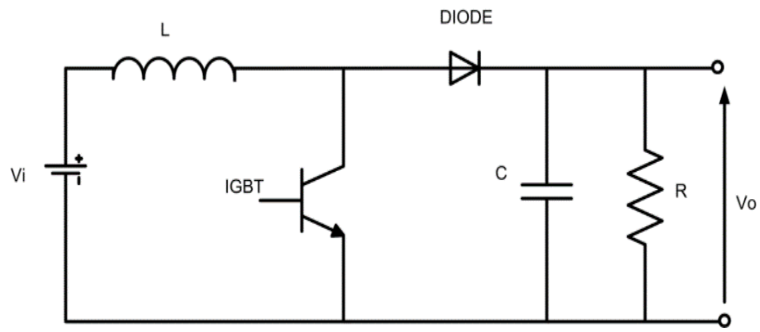

Figure 3.8: Boost converter circuit

The Figure 3.9 represents the main signals of a boost converter. PWM is the signal for the control stage and the voltage and the current in the inductance correspond to the power stage.

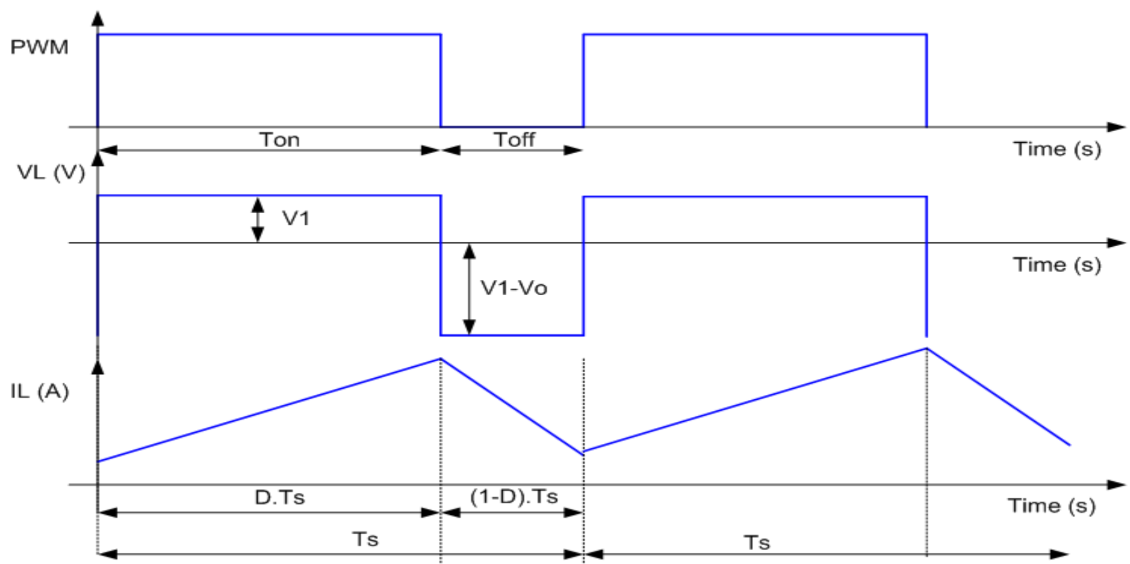

Figure 3.9: Boost converter signals

In this section before analyzing the complete mathematical analysis of the boost converter, the most relevant formulas are presented.

The voltage in the capacitor:

$$v_c = \int_{t1}^{t2} i_{c}dt \tag{3.3}$$

Where i_c is calculated since the relation between i_O and $i_L$current through the inductor is:

$$i_L = \frac{1}{L}\int_{t1}^{t2} v_L dt \tag{3.4}$$

Where v_L is equal to v_1 during T_{on} and $v_{L=}\ v_1 - v_0$ during T_{off}.

$$v_0 = v_i \frac{1}{1-D} \tag{3.5}$$

$$i_L = i_0 \frac{1}{1-D} \tag{3.6}$$

$$i_0 = i_L \text{ (1-D)} \tag{3.7}$$

Then, by using the equations from (3.3) to (3.7) the complete mathematical analysis of the boost converter can be calculated. The critical inductance that yields Continuous Conduction Mode is determined from the minimum value of inductor current I_{L-min} as:

$$L_C = \frac{D(1-D)^2 R}{2f} \tag{3.8}$$

In equation 3.9 "R" represents the load resistance. At least five DC homes will be consuming 2.5 kW of power almost entirely. Load in terms of resistance for five homes is calculated as follows:

$$R = \frac{V^2}{P} = \frac{48^2}{2500} = 0.9216\Omega \tag{3.9}$$

And, for a 50% duty cycle the critical inductance is calculated as follows:

$$L_C = \frac{0.5(1-5)^2 * 0.9218}{2*20*10^3} = 2.88\mu H \tag{3.10}$$

The duty cycle of the converter varies according to the weather and load conditions. Therefore, a higher value for the inductor is preferred to ensure that the converter is working in CCM mode at all time. The inductor of 20μH was tested and chosen to keep the converter in CCM mode under varying weather and load conditions [50], [51]. The output capacitor value is determined by:

$$C = \frac{D}{Rf} \times \frac{V_0}{\Delta V_0} \tag{3.11}$$

A 50% duty cycle at 25V input voltage will boost the output voltage to 50V, and the output capacitor required in this case would be:

$$C = \frac{0.5}{0.1884*20*10^3} * \frac{50}{1} = \frac{25}{3768} = 0.006635 \text{ F} \tag{3.12}$$

The output voltage ripple has an inverse relationship with the output capacitor value, so a lower output ripple will require a bigger capacitor. As mentioned, this converter will have varying duty cycle according to the different weather and load conditions. A 10mF capacitor was chosen for different operating conditions [51], [50].

Control of Boost Converter

With the variation of irradiation and temperature, the power output of PV module varies continuously. The maximum power point tracking (MPPT) algorithm is used for extracting the maximum power from the solar PV module and transferring that power to the load [48]. The optimal operation of the PV is ensured by the Incremental Conductance Maximum Power Point Tracking (MPPT) algorithm, fitting to rapidly changing irradiance conditions [49]. It aims "climbing" the typical hill-shaped P-V curve, pursuing the zero-slope condition:

$$\frac{\partial P}{\partial V} = 0 \tag{3.13}$$

The equation (3.13 in turns allows achieving the Maximum Power Point (MPP) when:

$$\left.\frac{\partial I}{\partial V}\right|_{\substack{i= I_{MPP} \\ v= V_{MPP}}} = -\frac{I_{MPP}}{V_{MPP}} \tag{3.14}$$

The MPPT regulates the PWM control signal of the DC – to – DC boost converter until the condition: (∂I/∂V) + (I/V) ¼0 is satisfied. In this method the peak power of the module lies at above 98 % of its incremental conductance. Therefore, the Flow chart of incremental conductance MPPT is shown in Figure 3.10 is used to drive the boost converter interfacing the PV system to the DC micro-grid.

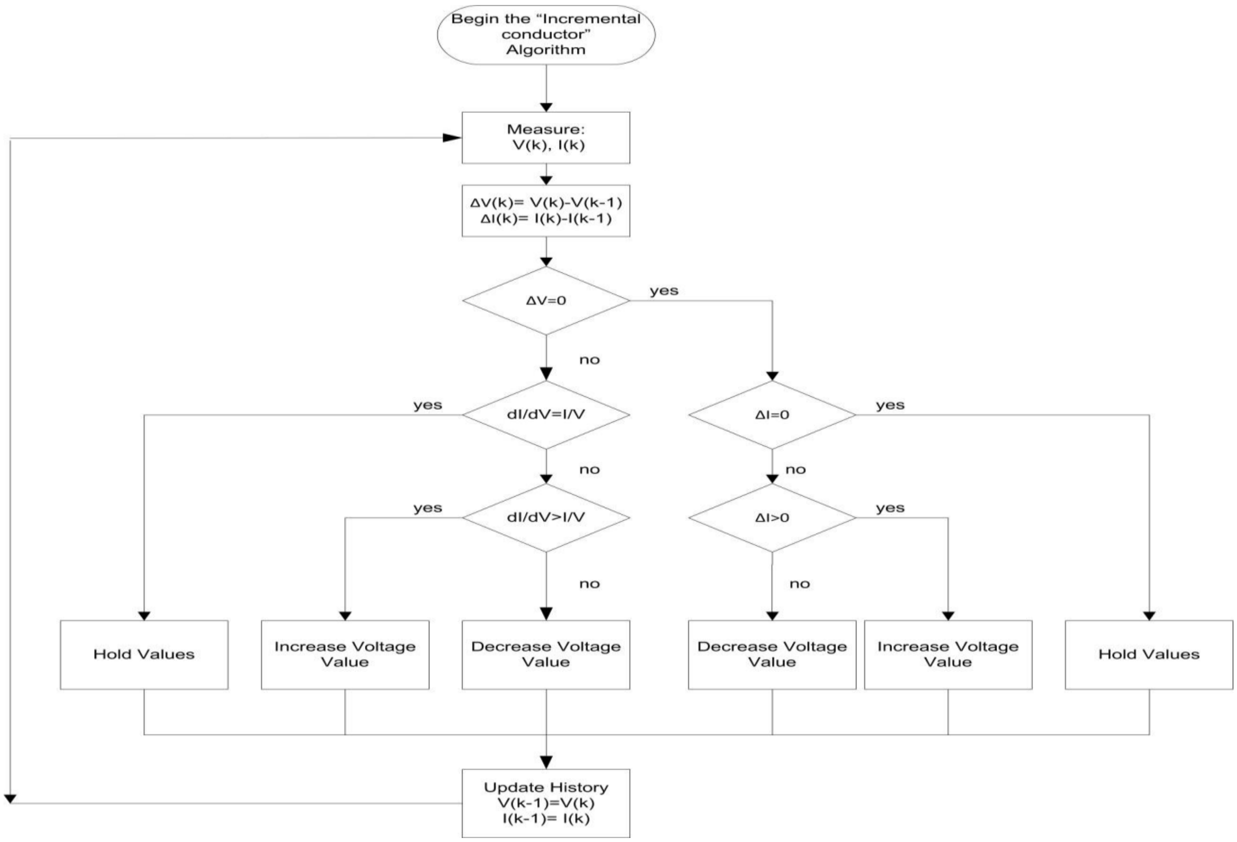

Figure 3.10: Flow chart MPPT for PV

Figure 3.11 shows the PV energy system configuration, where it is possible to see that the PV arrays are connected to the DC-DC boost converter.

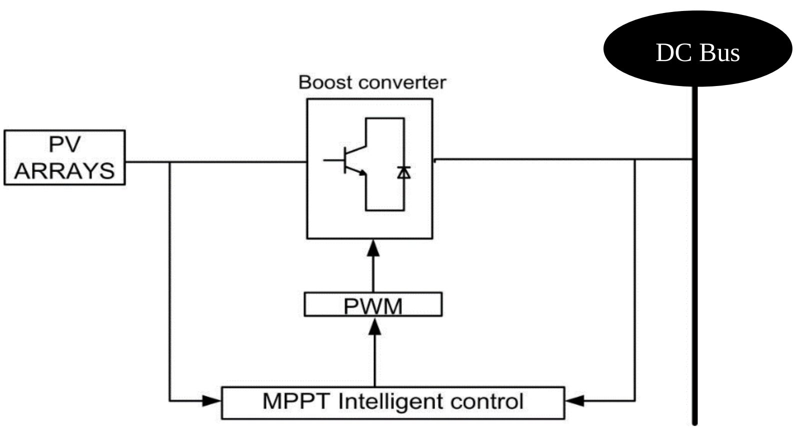

Figure 3.11: PV energy system

The PI controller used to drive the DC-DC converter for maximum power point tracking is illustrated in Figure 3.12. Instantaneous PV array voltage and current are measured to calculate the optimum operating voltage point

(V_{mmp}) of the PV array which generates the maximum power. The converter is controlled by the implementation of the MPPT algorithm.

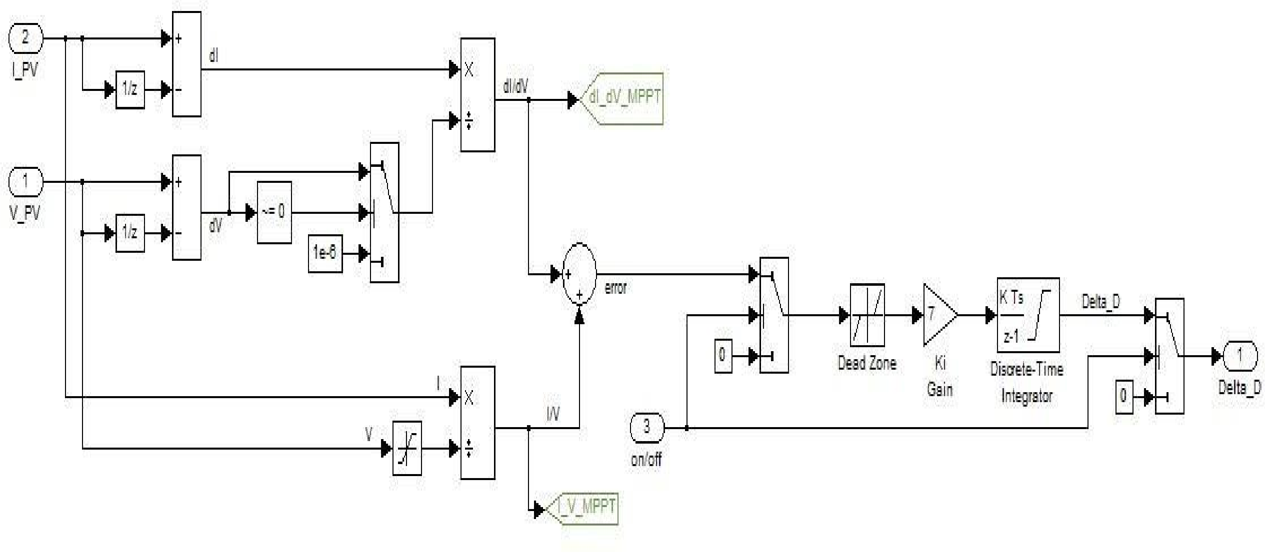

Figure 3.12: Boost control in PV system

3.3.2 Design, Modelling and Control of the Energy Storage System

PV power generation varies with the amount of sunlight shining on the panels at an instance, which results in lack of power generation during night time and cloudy weather. At such times, an energy storage is used to control the voltage level and the power flow through a bidirectional converter, in order to provide smooth power to the DC loads continuously. Chemical and electromechanical storages are a large part of ES as shown in Figure 3.13.

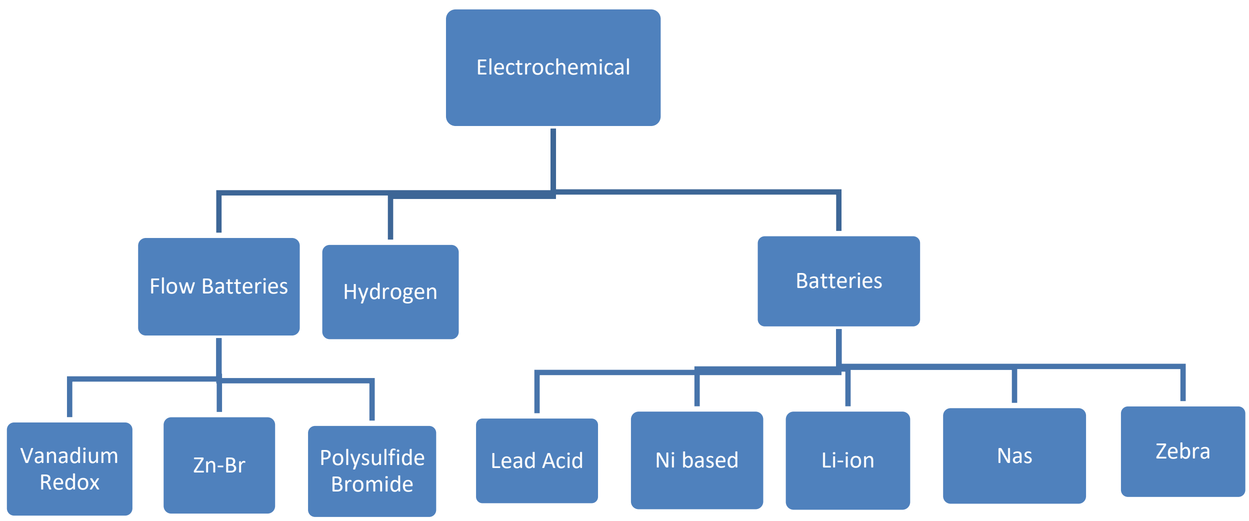

Figure 3.13: Electrochemical batteries classification [52]

Before the detailed description of the considered battery and the Simulink model for the battery is presented, some characteristic parameters of the battery which is discussed in the following section and apply to the DC micro-grid defined for clarity as follows:

- **Power Capacity**: is the maximum instantaneous output that an ES device can provide, usually measured in kilowatts (kW) or megawatts (MW).
- **Energy Capacity***:* is the amount of electrical energy the device can store usually measured in kilowatt-hours (kWh) or megawatt-hours (MWh).
- **Response Time***:* is the length of time it takes the storage device to start releasing power from the moment it is activated.
- **Efficiency:** indicates the quantity of electricity which can be recovered as a percentage of the electricity used to charge the device.
- **Round-Trip Efficiency***:* indicates the quantity of electricity which can be recovered as a percentage of the electricity used to charge and discharge the device.

3.3.2.1 Modelling of The Energy Storage System

Lead Acid Model

Among batteries which are used in renewable energy storage systems, lead acid battery is the most common one. Even though this type of batteries has a low energy density, moderate efficiency and high maintenance requirements, they have a significantly long lifespan, fast response and low costs compared to other battery types. One of the singular advantages of Lead-acid batteries is that they are the most commonly used form of battery (for short-term applications that need discharging time in the range of seconds but also for long-term application with discharge time in the range of hours) and therefore, have a well-established, mature technology base.

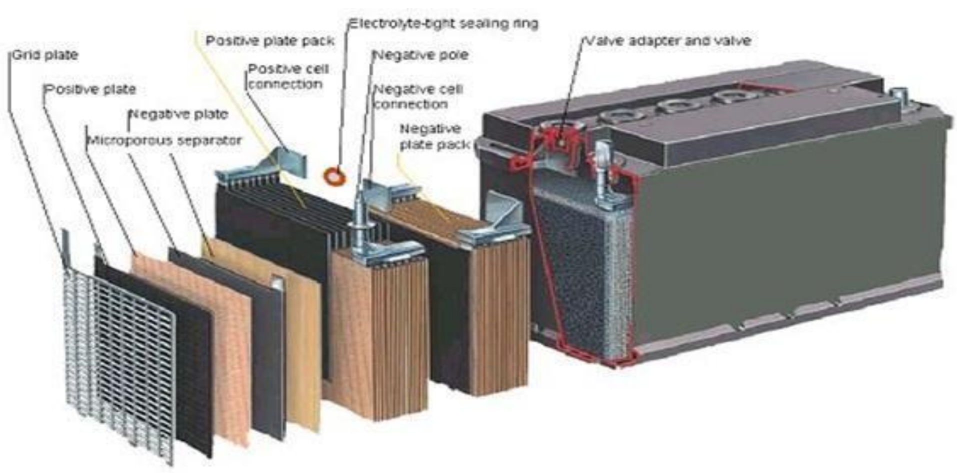

Figure 3.14: Lead Acid Battery. Source: The battery rejuvenator website

Lead-Acid batteries are electrochemical cells based on chemical reactions involving lead and sulphuric acid. Both the power and energy capacities of lead-acid batteries are based on the size and geometry of the electrodes. The power capacity can be increased by increasing the surface area for each electrode, which means greater quantities of thinner electrode plates in the battery. Though, to increase the storage capacity of the battery, the mass of each electrode must be increased, which means fewer and thicker plates. The storage capacity required for the battery bank depends on the number of days batteries can provide power to the load without recharging. Depth of Discharge (DOD) is the amount of energy drawn from a battery compared to its total storage capacity. For a PV system, two common terms related to DOD are maximum DOD and average daily DOD. Maximum DOD is the maximum amount of charge that can be drawn out of the battery. It is also related to the autonomy capacity required to operate the system loads or given number of days with no generation from PV.

A system designed with very low DOD will have most of the battery energy available to the load but with a trade-off for longer battery life. The average daily DOD is the amount of energy drawn from battery's full capacity with the average daily load profile. A system designed for longer autonomy periods (more capacity) will have lower average daily DOD. For this system, DOD of 80% is selected, which is typical for isolated PV storage systems. A lead-acid (LA) battery set of typical parameters observed in Table 3.4.

Table 3.4: Typical parameters of LA battery

Specific energy	30-40 $^{Wh}/_{Kg}$
Energy density	60-75$^{Wh}/_{Litter}$
Specific power	About 250 $^{W}/_{Kg}$
Nominal cell voltage	2 V
Electrical efficiency	About 80%, depending on recharge rate and temperature
Recharge rate	About 8 hours (possible to quick recharge 90%)
Self-discharge	1.2% per day
Lifetime	About 800 cycles, depending on the depth of cycle

Advantages

Unlike most batteries, Lead Acid battery can be used as energy storage for both short and long-term applications which in return has significant contribution for the success of this project design and implementation. In addition, the minimum capital cost of the battery as a result of maturity in the market is another advantage.

Disadvantages

Lead Acid batteries are tremendously(highly) sensitive to the environment, especially to the temperature. The typical operating temperature is about 27°C, but a change in temperature of 5°C or more can cut the life of the battery by 50% [53]. The lifetime of this kind of batteries is a crucial in determining appropriate materials for our system. Apart from the effect of temperature Lead Acid batteries depend strictly to the DOD (depth of discharge). For DOD in the range of 2-5 %, typically, the lifetime in cycles of this battery is equal to 1000, with deep DOD this value decreases to 300-500 cycles. This is one of the shortcoming of the lead acid. Moreover, due to the high density of the materials used in these batteries, the characteristic energy densities are low, and also the efficiency compared with other kind of energy storage, is not so high. At last, the lead is toxic and for this reason it has to be recycled. Similarly, the sulphuric acid in the battery used as the electrolyte is corrosive and when overcharged the battery generates hydrogen which dowries an explosion risk.

Applications

Because of the low cost, this type of energy storage is used basically for power quality, UPS and some spinning reserve applications. Theoretically it can be used also for long term applications like energy management but in reality, this application is limited by the short lifespan.

Battery Bank MATLAB Implementation

The battery is modeled by a controlled voltage source in series with a constant resistance, as shown in Figure 3.15.

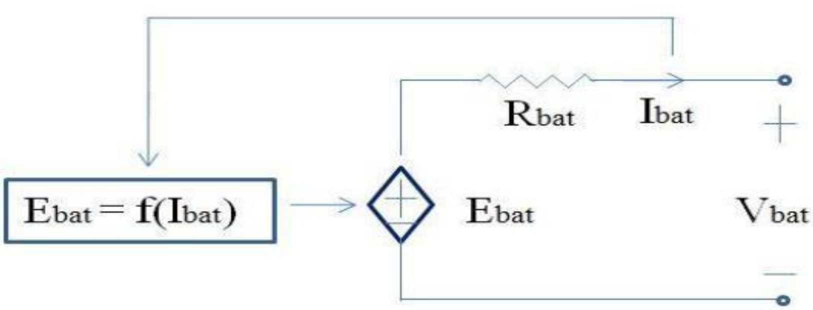

Figure 3.15: Battery equivalent circuit diagram

This basic equivalent battery circuit is represented by shepherd's equation as:

$$E_{bat} = E_0 - K\frac{(1-SOC)}{SOC} * Q + Ae^{-B(1-SOC)Q} \quad (3.15)$$

The voltage at the battery terminal is calculated as:

$$V_{bat} = E_{bat} - R_{bat} * I_{bat} \quad (3.16)$$

where:

E_{bat}: internal voltage (V)

E_0: battery voltage constant (V)

K: polarization constant (V/Ah) or polarization resistance (Ω)

SOC: State of charge (%)

Q: battery capacity (Ah)

A: exponential Zone amplitude (V)

B : exponential zone time constant inverse (1/Ah)

V_{bat}: terminal voltage (V)

I_{bat}: battery current (A)

The Simulink battery model available in MATLAB, is depicted in Figure 3.16:

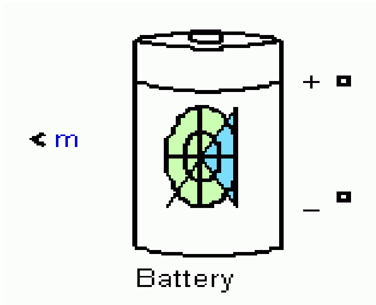

Figure 3.16 Simulink battery block

The Simulink battery block implements a generic dynamic model parameterized to represent most popular types of rechargeable batteries.

Where:

- **m** : The current of the battery, input signal and SOC, output signal.

As discussed in the previous section, lead-acid battery type is the optimum choice for the isolated PV backup system. The sizing of the lead-acid model is done in the next section.

3.3.2.2 Battery Bank Sizing for off-grid DC Micro-grid

Calculating the number of batteries needed for the DC micro-grid (isolated PV energy storage) system mainly depends on the days of autonomy desired. Days of autonomy are the number of days a battery bank will supply a given load without being recharged by a PV array or another source. For critical loads 2 to 3 days of autonomy are recommended. If the load being supplied is not critical then 1 autonomy day is commonly used. A critical load is a load that must be used all the time [54].

Another important factor is the maximum depth of discharge of the battery. The depth of discharge refers to how much capacity will be used from the battery. Most systems are designed for regular discharge values between 40 to 80 percent [54]. Hence, and according to [55], the required battery bank capacity (B_{C-R}) for a solar-battery renewable energy (DC micro-grid) system can be calculated as follow:

$$B_{C-R} = \frac{I_C N_D}{M_{DOD}} \tag{3.17}$$

Where I_C is the Amp-hour consumed by the load in a day (Ah/day), N_D is the number of autonomy days, and M_{DOD} is the maximum depth of discharge. The number of batteries to be connected in parallel (N_{B-P}) to reach the Amp hours required by the system can be calculated as follow [54]:

$$N_{B-P} = \frac{B_{C-R}}{B_C} \tag{3.18}$$

Where B_C is the capacity of the selected battery(Ah). While, the number of batteries to be connected in series (N_{B-S}) to reach the voltage required by the system can be calculated as follow [54]:

$$N_{B-S} = \frac{V_S}{V_B} \tag{3.19}$$

Where V_S is the DC system voltage (V) and V_B is the battery voltage (V).
As per the above reasons, the Lead-acid battery with Carbon-enhanced Electrodes has been chosen to implement the Economical Storage Management, because the other technologies are not benefitting to be implemented for

an optimal participation with the system. Hence, for the battery bank, Lead-acid battery with Carbon-enhanced Electrodes is selected (Appendix D), which has 520A of capacity with 12V terminal voltage.

Now let's size a battery bank needed to supply 34,000Wh per day to a DC electric load of Tullu Gudo Island.

- The DC voltage of the battery bank is 48V.
- Nominal voltage of the battery rating is 40.
- The number of autonomy days is 2 days.
- The maximum depth of discharge is 60%.
- The selected rechargeable battery is (12V-520Ah) Lead-acid battery with Carbon-enhanced Electrodes.

The battery bank rating calculated as follows:

$$\text{Battery rating} = \frac{2.5\ \text{KW x 48hr}}{40\text{V x 0.6}} = 5000\text{Ah}$$

Then, by using the equations from (3.17) to (3.19) the batteries required by this system can be calculated as follows:

$$\text{Watt-hour capacity of battery bank} = \frac{{}^{Wh}/_{day}\ x\ \text{N}_\text{D}}{\text{M}_\text{DOD}} = \frac{34{,}000\ \text{x}\ 2}{0.6} = 125{,}800\text{Wh}$$

Dividing the above result by system voltage. Result is the minimum Amp-hour(Ah) capacity of battery bank as follows:

$$\text{B}_{\text{C}-\text{R}} = \frac{125{,}800\text{Wh}}{48\text{V}} = 2620.8333 \approx 2621\text{Ah}$$

$$\text{Number of battery in parallel}(\ \text{N}_{\text{B}-\text{P}}\ ) = \frac{\text{B}_{\text{C}-\text{R}}}{\text{B}_\text{C}} = \frac{2621}{520} = 5$$

$$\text{Number of battery in series}(\text{N}_{\text{B}-\text{S}}) = \frac{\text{S}_\text{V}}{\text{B}_\text{V}} = \frac{48}{12} = 4$$

Hence, 5000Ahr battery rating of (12V-520Ah) Lead-acid battery with Carbon-enhanced Electrodes is considered and, consequently, 4 and 5 numbers of batteries are required to connect in Series and parallel respectively.

3.3.2.3 Control of Energy Storage System

Bidirectional DC/DC converter

The DC/DC converters are circuits that have input and output DC voltage with different values. Actually, the output is an average value, and Figure 3.17 shows the general system of this converter topology.

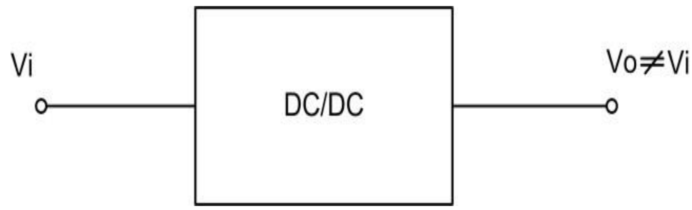

Figure 3.17: General system DC/DC converter

The specific converter used with these batteries has the bidirectional buck-boost configuration. In this thesis, the DC micro grid is connected to a battery bank through bidirectional converter; It is able to work as a buck (step-down) when the battery has been charged and as a boost (step-up) in the case the battery has been discharged and discharge/charge current from/to DC micro grid. Figure 3.18 shows the circuit of the used converter. It works in two modes: charged mode and discharged mode.

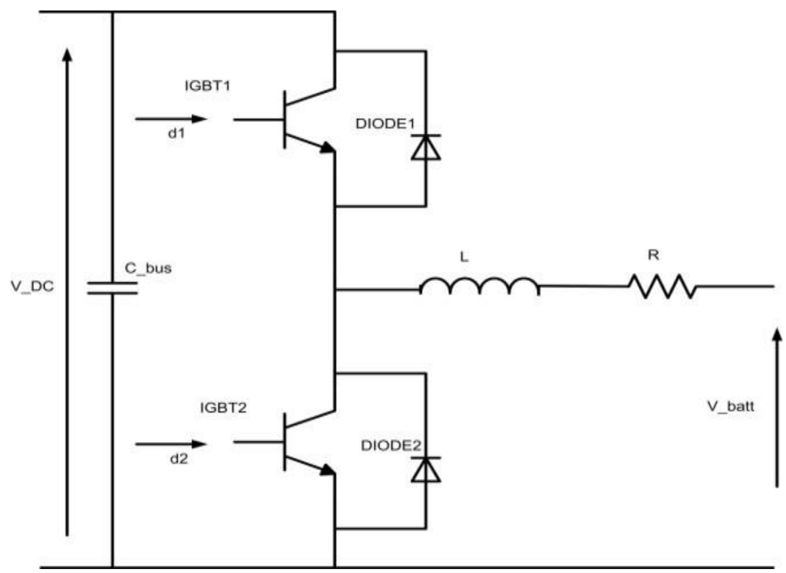

Figure 3.18: DC/DC bidirectional converter configuration

In charge mode, the upper IGBT1 is on and it is controlled through PWM signal d, at the same time the lower IGBT2 is off. In this time the converter keeps the voltage level on the micro-grid at 48V and it is able to supply the battery until it is charged.

In discharge mode, the lower IGBT2 is on and it is controlled through PWM signal, at the same time the IGBT1 is off in this time the converter keeps the voltage level on the micro-grid at 48V, it is able to supply the DC-bus and the battery is discharging. This converter configuration is able to supply a negative or positive current on the base of discharge or charge of the battery respectively, while the voltage level is always positive.

Analyzing the converter circuit is clear to see that it is consisting of two choppers (IGBT/DIODE) properly connected. The control of these two IGBTs is complementary, so when one is conduced the other one is off, so never the DC-bus is affected of a short circuit ($V_{DC} = 0$). The behavior of the converter to switch on the two modes should be interesting, so the battery is able to discharge the following condition is necessary:

$$V_m > 0 , I_m > 0 \tag{3.20}$$

thus, the upper chopper is working, in the other way the battery is able to charge on these conditions:

$$V_m > 0 , I_m < 0 \tag{3.21}$$

thus, the lower chopper is working.

Control of Bidirectional DC/DC Converter.

The main objective of the bidirectional converter controller is to control the ES, to maintain a constant dc-bus voltage, i.e. on the DC micro-grid. To have this, two loop control circuits are proposed, the first one is to control the voltage and the second one is to control the current. So, the following control is implemented (Figure 3.19), where the loops have to perform the control of voltage and current through the PI controls.

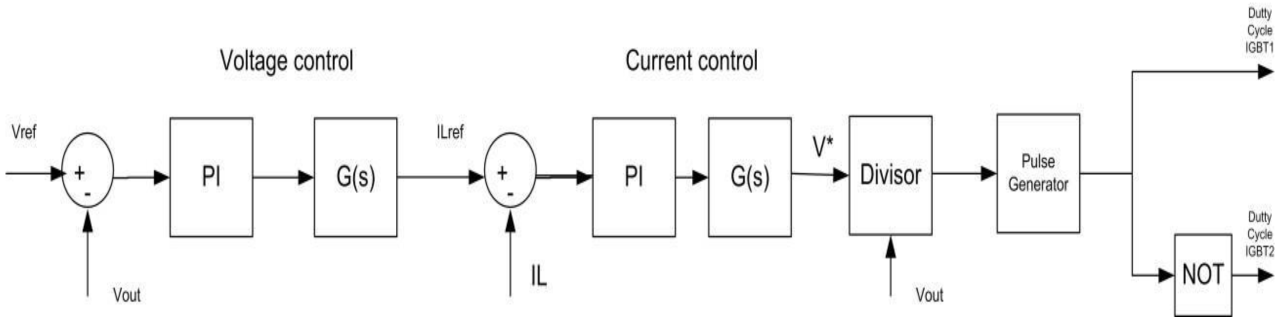

Figure 3.19: Scheme of bidirectional converter control

The first loop allows having the average voltage value on the DC-bus on 48V, but without the second loop, the low oscillations on the average voltage value increase and the system will be instable. So, to have a stable system the second loop is needed, thus the oscillations are removed and the voltage on the DC load is kept constant.

The values of K_P and K_i on both the PI controls are calculated considering the transfer functions G1(s) and G2(s) and by using the SISO tool in MATLAB for the following buck-boost circuit in Figure 3.20 in small signal analysis.

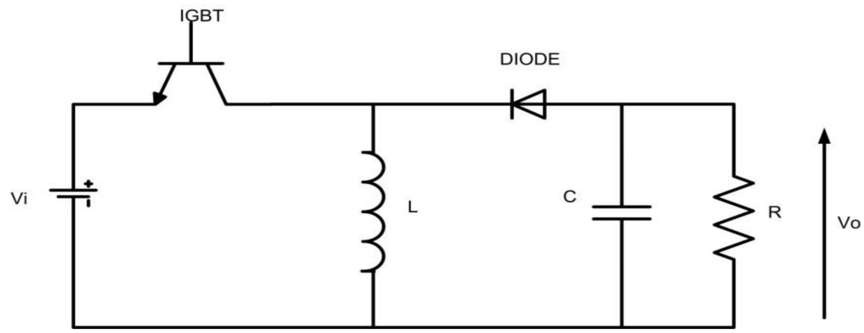

Figure 3.20. Schematic of the buck-boost converter

For the buck-boost converter the line-to-output G1(s) and control-to-output G2(s) transfer functions are given from the literatures [51], [50] and they are calculated by following:

$$G_1(s) = \frac{V}{DD'} \frac{1 - s\frac{DL}{D'^2 R}}{\text{dem}(s)} \tag{3.22}$$

$$G_2(s) = \frac{D}{D'} \frac{1}{\text{dem}(s)} \tag{3.23}$$

Where dem(s) = $1 + S\frac{L}{D'^2 R} + S^2 \frac{LC}{D'^2}$,D = $\frac{Vo}{Vo - Vi}$ is the duty cycle and D'= 1-D

Where

D = duty cycle

V_0 = output voltage

V_i = input voltage

The PI controller used to drive the bidirectional DC-DC converter is illustrated in Figure 3.21.

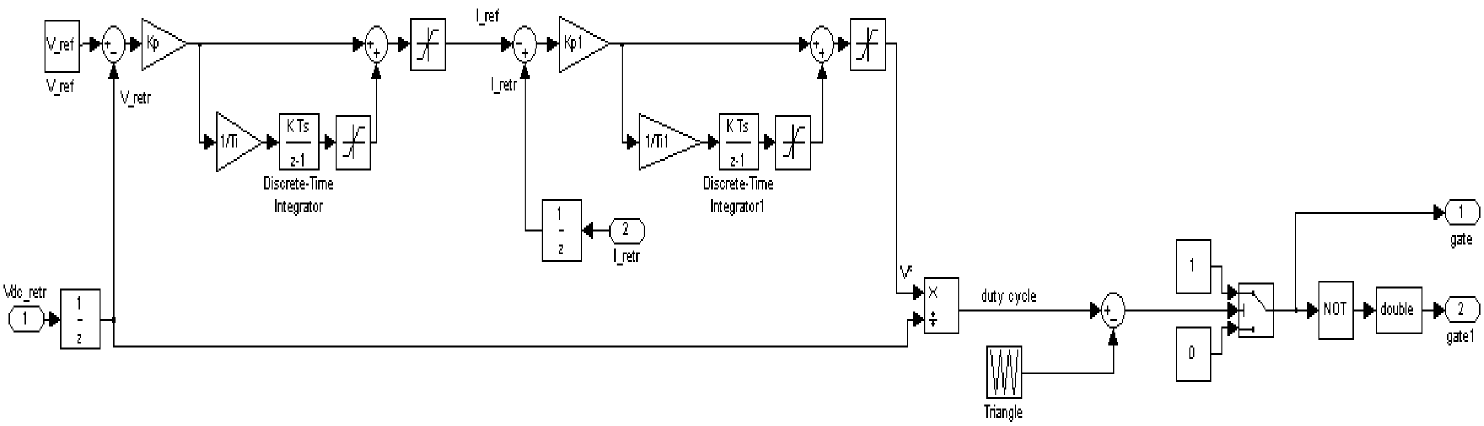

Figure 3.21: Bidirectional DC-DC converter controller

3.3.3 Load Side Distribution Network

The load side is where the generated energy is distributed between three appliance circuits inside the DC Home. From the 48V distribution network, the power is distributed to the loads inside the home by means of circuit breakers. Appliances are spread apart as evenly as possible into three circuits, where appliances are connected in shunt form. Figure 3.21 shows the general load side distribution at a high level; this does not show exact configurations of circuit breakers and appliances. Figure 3.22 is a continuation of Figure 3.5. A single DC home load can be varied from 100-500W.

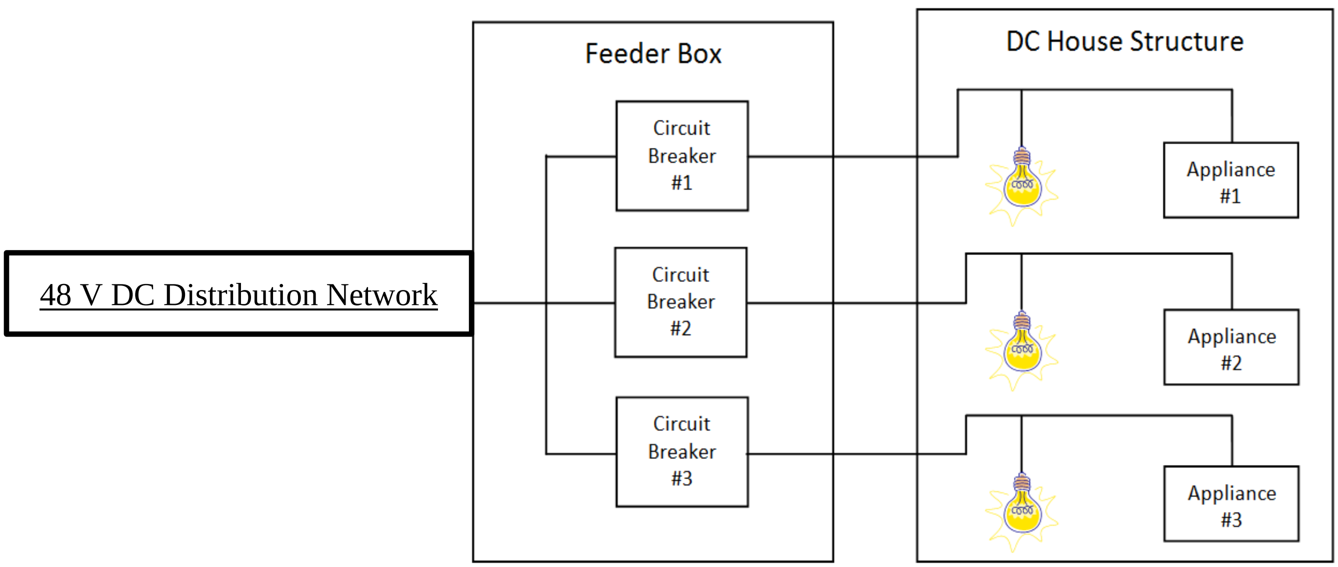

Figure 3.22: Block diagram of load side

Feeder Box Panel

The feeder box is a panel located on the outside of the DC House and contains the 48V DC distribution panel and circuit breakers.

DC Power Distribution Panel

The DC distribution panel for the DC House must be able to connect the 48V system bus to three circuit breakers, which will be connected to three branch circuits to power the appliances inside the home.

Circuit Breakers

Power is distributed among the three appliance circuits via the DC distribution panel, which contains three circuit breakers. These circuit breakers protect the system from inrush (input surge) current caused by the loads inside the DC House. These circuit breakers are very important for protection of the system. Appliances will be shunt-connected to one of three branch circuits inside the DC House. Therefore, since current add up when loads are placed in parallel, the DC circuit breakers are chosen based on the maximum current required to power the appliances on a certain branch. The goal here is to choose a circuit breaker size just above this maximum current rating so that it trips and open-circuits that particular branch if a short circuit occurs. Another goal is to evenly split up the appliances between the three circuits based on their current ratings so that the three circuit breakers can have the same current rating. The current on each branch is 12A. Figure 3.23 shows the power flow in a basic DC circuit. The power loss in a DC circuit is directly proportional to the conductor resistance and the amount of current flowing through the conductor as shown by following equation:

$$P_{loss} = P_{source} - P_{load} = V_{DC}I - V_2 = I^2R \tag{3.24}$$

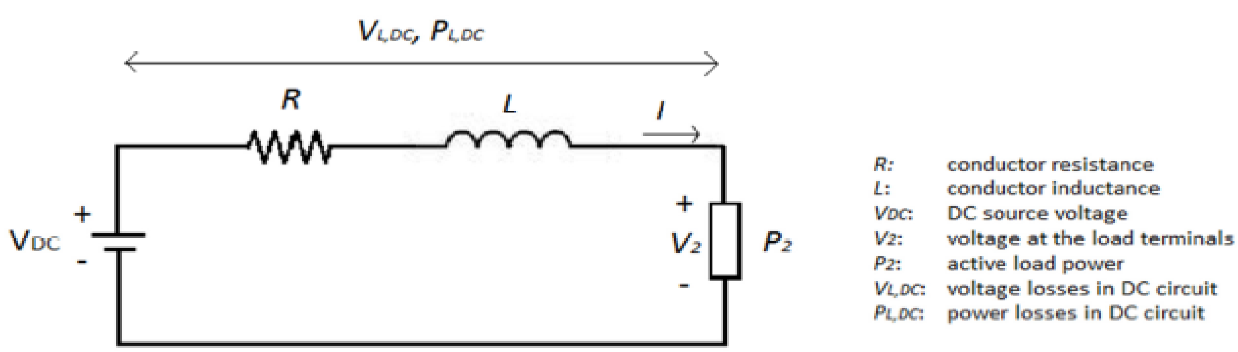

Figure 3.23: DC equivalent circuit diagram [58]

At full load, the minimum current for one DC home is:

$$I_{full-load} = \frac{P}{V_{DC-Bus}} = \frac{500W}{48V} = 10.4167$$

At full load, the minimum current for five (5) DC homes is:

$$I_{full-load} = \frac{P}{V_{DC-Bus}} = \frac{5*500W}{48V} = 52.08333A \tag{3.25}$$

Equation 3.25 shows distribution network will have high currents due to the low distribution voltage, therefore minimum resistance is desired in the distribution conductors in order to minimize distribution loses. Round conductors are measured by using an American Wire Gage (AWG). One specialized overhead power-line conductor is the aluminum-conductor steel-reinforced (ACSR) type used for long-distance electrical power transmission. This type of conductor has stranded aluminum wires. Their performance is highly reliable for many years even under adverse weather conditions. Table 3.5 shows the size of copper and aluminum conductors. RH Copper conductor at 10 AWG size is selected for the distribution network based on the ampacity rating, DC resistance, and cost and 18 AWG size is selected to connect a single DC House to the distribution network.

Table 3.5: Size of copper and aluminum conductors.

Size (AWG or MCM)	Area = D^2 Area (cmil)	Number of Wires	Diammeter of Each Wire	DC resistance (in.) (ohm/ 1000ft) 25°C Copper	Aluminum
18	1,620	1	0.0403	6.51	10.7
16	2,580	1	0.0508	4.1	6.72
14	4,110	1	0.0641	2.57	4.22
12	6,530	1	0.0808	1.62	2.66
10	10,380	1	0.1019	1.018	1.67
8	16,510	1	0.1285	0.6404	1.05
6	26,240	7	0.0612	0.41	0.674
4	41,740	7	0.0772	0.259	0.424
3	52,620	7	0.0867	0.205	0.336
2	66,360	7	0.0974	0.162	0.266
1	83,690	19	0.0664	0.129	0.211
0	105,600	19	0.0745	0.102	0.168
0	133,100	19	0.0837	0.0811	0.133
0	167,800	19	0.094	0.0642	0.105
0	211,600	19	0.1055	0.0509	0.0836
250	250,000	37	0.0822	0.0431	0.0708
300	300,000	37	0.09	0.036	0.059
350	350,000	37	0.0973	0.0308	0.0505
400	400,000	37	0.104	0.027	0.0442
500	500,000	37	0.1162	0.0216	0.0354
600	600,000	61	0.0992	0.018	0.0295
700	700,000	61	0.1071	0.0154	0.0253
750	750,000	61	0.1109	0.0144	0.0236
800	800,000	61	0.1145	0.0135	0.0221
900	900,000	61	0.1215	0.012	0.0197
1000	1,000,000	61	0.128	0.0108	0.0177

The DC resistance of the conductors leads to voltage drop in the network that varies with the distance and the amount of current flowing in the cable $(V_{drop} = I * R_{cable})$. Thus, DC-DC converters with PI controllers are required at strategic locations in the distribution network in order to boost the voltage back to 48V.

Chapter 4

Simulation Results & Discussion

4.1 Introduction

The objective of the simulations is to verify that the proposed off-grid DC micro-grid simulation model can operate in off-grid mode, and to analyze the performance of the system in different scenarios. The proposed model of the off-grid DC micro-grid is shown in Figure 4.1. The proposed off-grid DC micro-grid simulation model has been implemented by MATLAB/Simulink and in this chapter, will be shown the results.

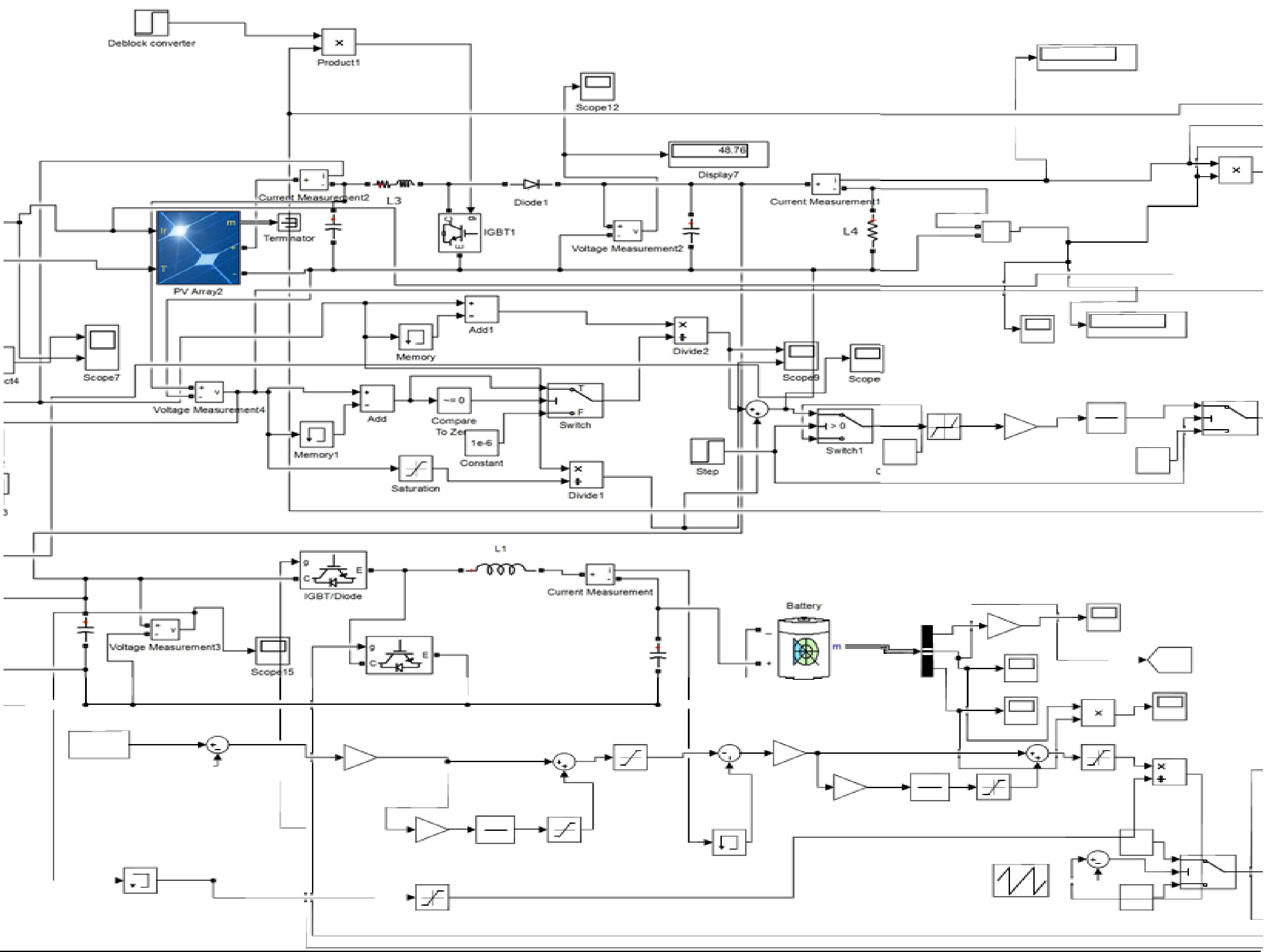

Figure 4.1. Implemented off-grid DC micro-grid by Simulink

4.2 Simulation Results

The DC micro-grid is proposed to work in off-grid mode, where the ESS acts as the "master", to control the voltage level on the DC bus and to balance the power flow. In this scenario the input of the PV is the fluctuation of the irradiance in PV unit and in this unit the MPPT method is implemented which is illustrated in the section 3.3.

In this study, the irradiance value and the power generated by the PV array constant as illustrated in Figure 4.2. The generated power reaches the nominal value when the irradiance is 800 W/m^2. Therefore, the MPPT control works properly to allow the model to supply the maximum power for every irradiance value. This MPPT control has been explained in section 3.3.

Figure 4.3 illustrates the comparison between ${dI}/{dV}$ and ${I}/{V}$. Where the error is near to zero during the entire region except some noise can be observed. This is because when the steady state is reached in the system, the algorithm oscillates around the peak point and so some noise is introduced to the outputs.

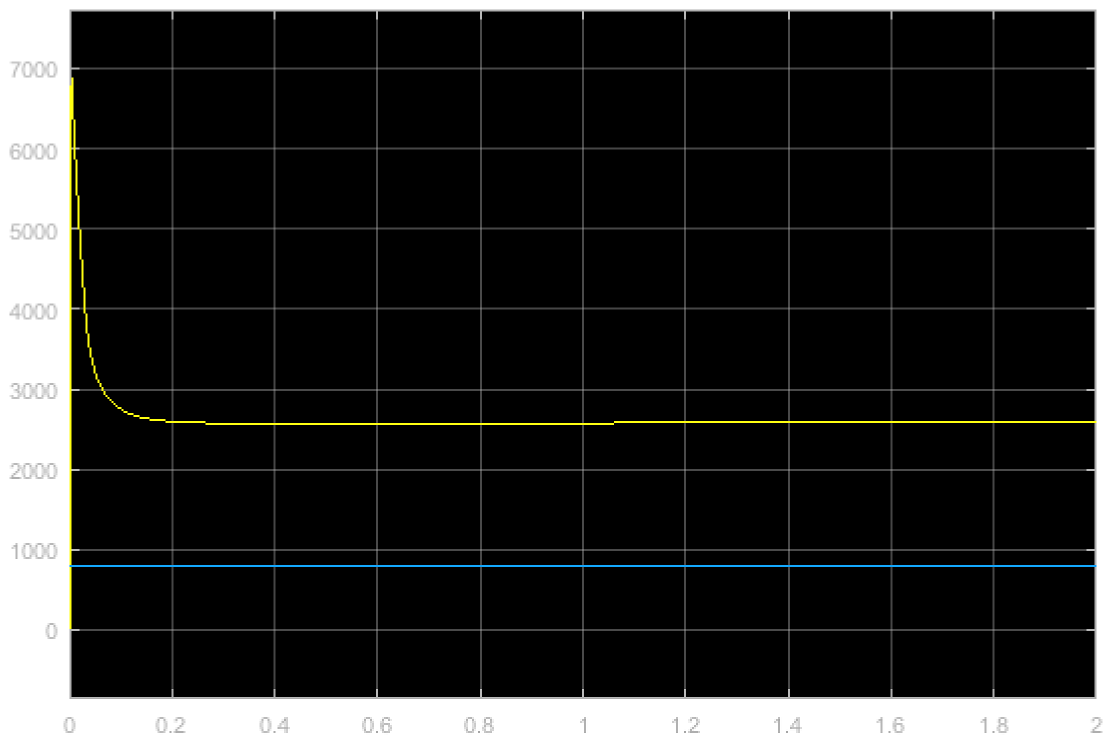

Figure 4.2: Comparison between power generated by the PV top(yellow), and irradiance value(blue) bottom

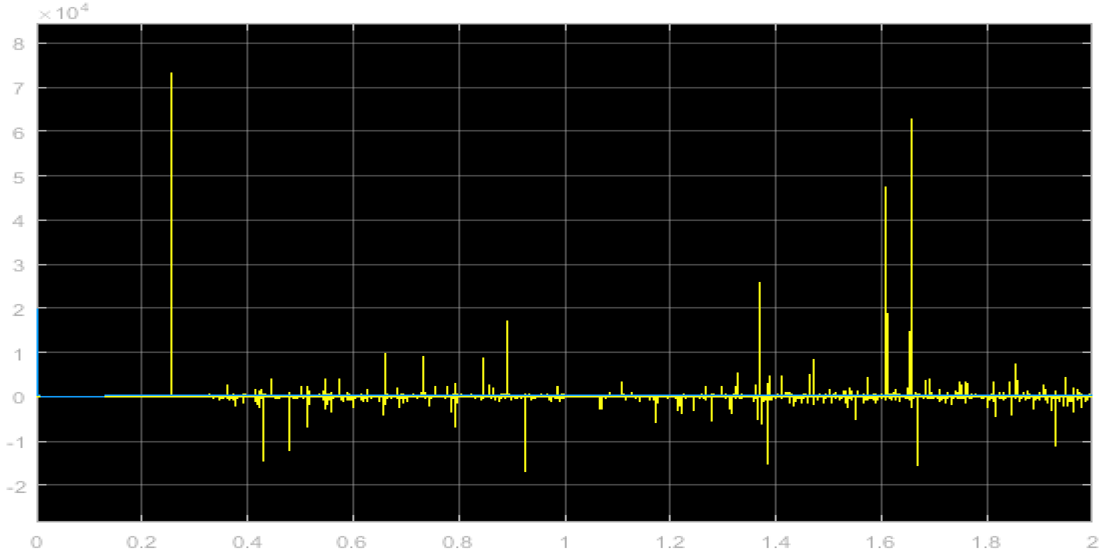

(a)

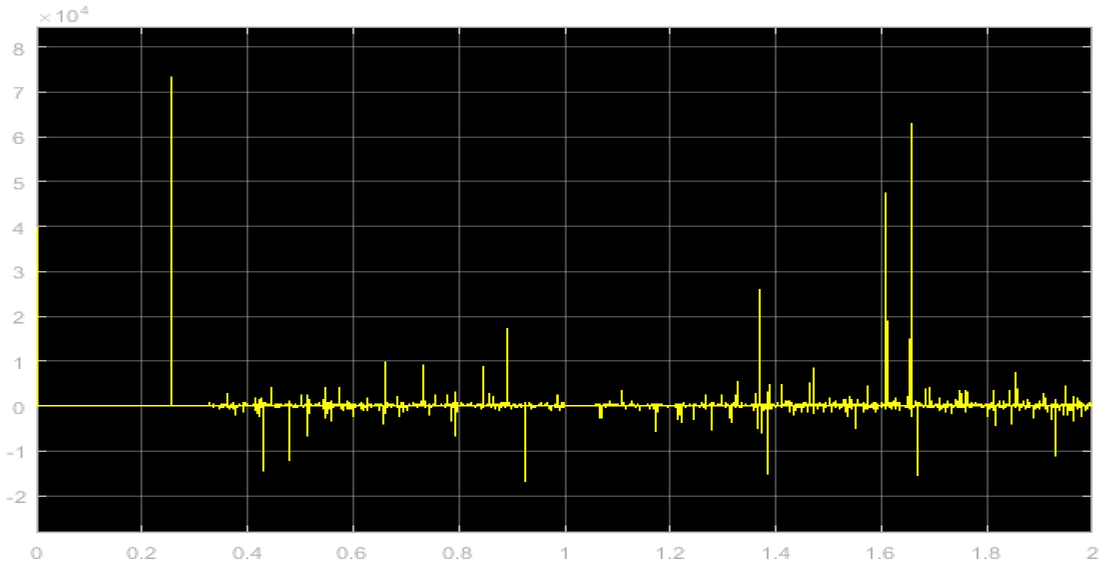

(b)

Figure 4.3: Control of the PV MPPT mode. (a) Comparison between dI/dV (yellow) and I/V (blue) b) Error

As discussed earlier, the ESS controls the power flow and the DC voltage bus. The reference voltage has been chosen in chapter 2, with a value of 48V. The comparison between the DC bus voltage and the reference voltage is shown in Table 2.1. The ESS remains the voltage value at 48V. The ESS controls the power flow on the micro-grid shown in Figure 4.4 by injecting and consuming power by the bi-directional converter to remain the supplied power at 2.5kW. The power flow in the DC system is displayed in Figure 4.4. Here it is interesting noticing the ESS cope with the power unbalance passing from charging to discharging mode. Figure 4.5 illustrates the voltage of the batteries. The voltage on the batteries increase when the ESS is charging, and discharge energy to balance the power flow. The SOC value changes slightly due to the limited time simulation.

To be able to show a completely discharge cycle the simulation time has to be longer than one hour.

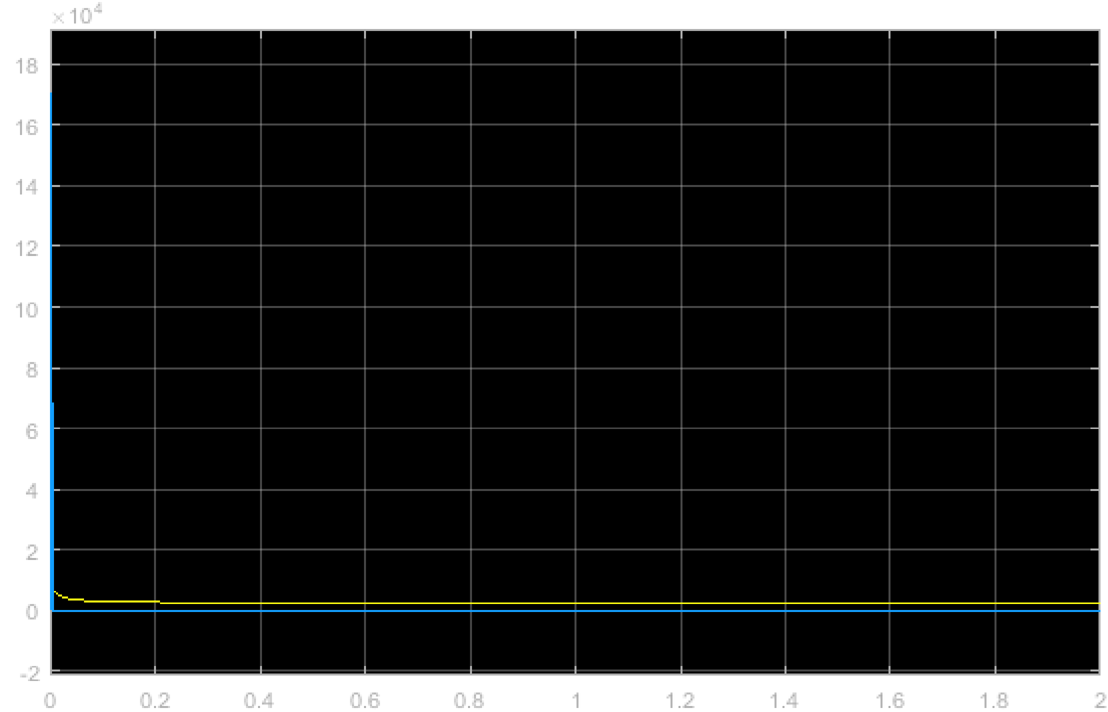

Figure 4.4: Power flow in the off-grid DC micro-grid: Power of ESS(Blue) and Pload(Yellow)

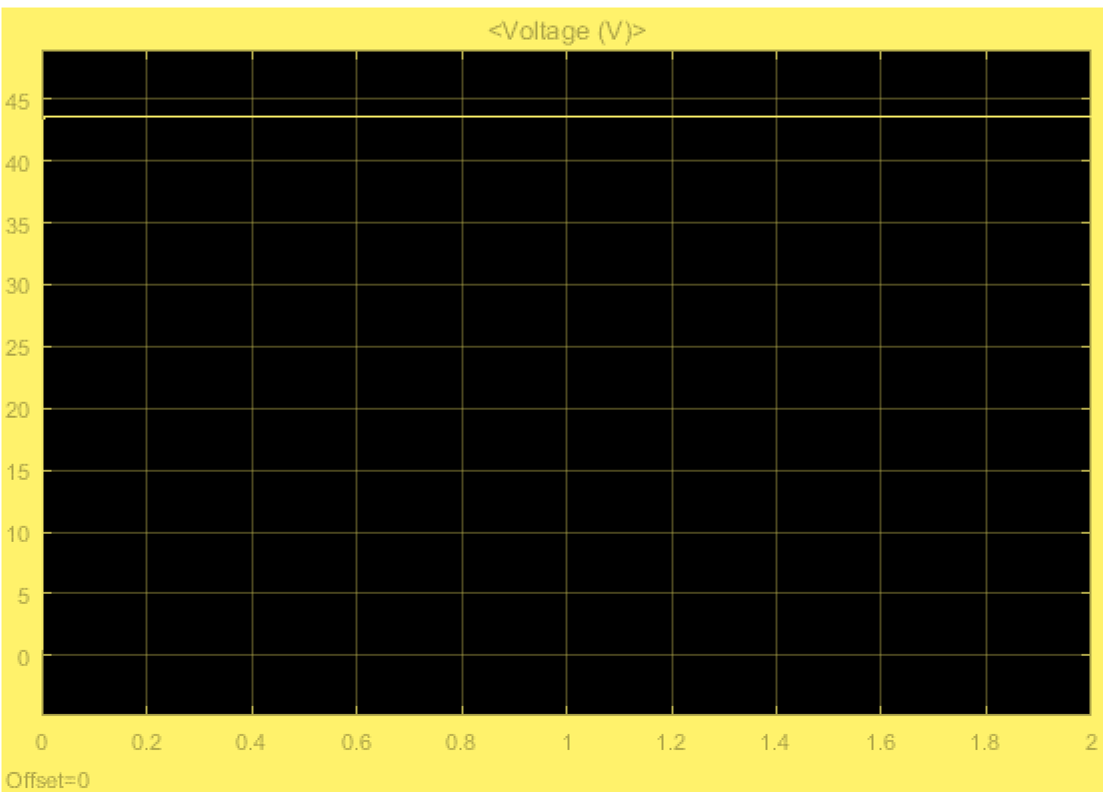

Figure 4.5: ESS characteristics: Voltage of the battery

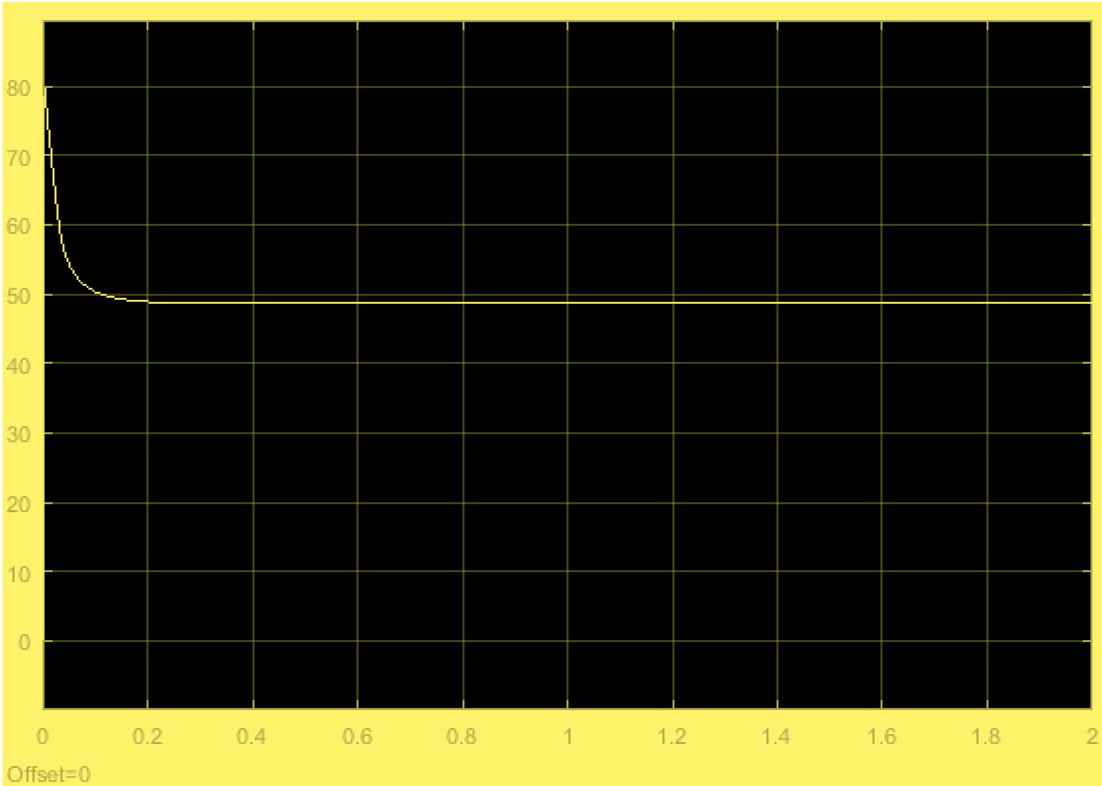

Figure 4.6: DC voltage level on the off-grid DC micro-grid

Finally, the simulation results show the performance of the proposed design, modelling and control of off-grid DC micro-grid for DC homes. The voltage in the DC micro-grid is shown in Figure 4.6, which is constant and fixed at its reference; the PV maximum power is extracted; and the ESS is perfectly controlled and balanced the voltage level on the DC bus and the power flow. Thus, the result shows that this paper achieved the objective which is designing and modelling of off-grid DC micro-grid for five (5) DC homes.

Chapter 5

System Cost Analysis

5.1 Introduction

The major factor driving the growth of the renewable energy sources such as photovoltaic, wind is their competitive cost, which has been decreasing for the past two decades. The DC distribution method is chosen for the study because it is more efficient and requires fewer components than an AC distribution method. In the following sections, a DC vs. AC distribution cost analysis is performed for a system that could range from 1kw to 50 Kw particularly for a DC power rating of 2.5Kw for five (5) DC homes of the study area.

5.2 PV Array and MPPT Charge Controller Cost

BP Solar SX3190W solar module is selected for the system due to its competitive price per watt (Appendix B). Table 5.1 summarizes the cost for a system ranging from 1kW to 50kW with 85% and 75% system efficiencies. The data from the table are plotted in Figure 5.1. The plot shows that improving the system efficiency is significant in reducing the high initial cost for a PV system.

Table 5.1: Summary of PV cost for 85% and 75% system efficiency

System KW	85% eff	75% eff
1	$2,868.24	$3,255.84
2.5	$7,170.60	$8,139.60
5	$14,341.20	$16,279.20
7.5	$21,511.80	$24,418.80
10	$28,682.40	$32,558.40
20	$56,977.20	$64,729.20
30	$85,659.60	$96,900.00
40	$113,954.40	$129,070.80
50	$142,249.20	$161,241.60

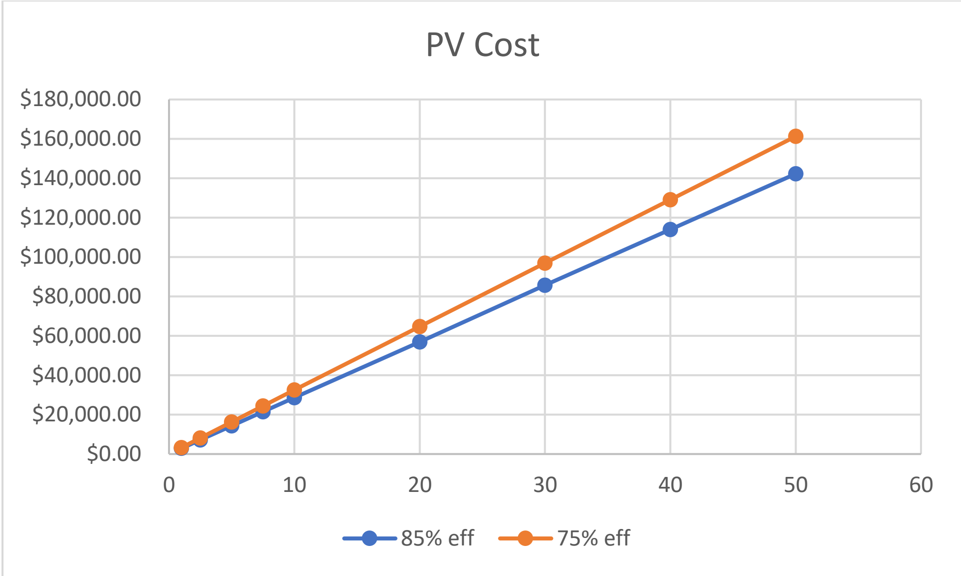

Figure 5.1: DC Distribution system PV cost with 85% and 75% efficiency

The MPPT charge controller selected for the system is Outback FM-80 Flexmax (Appendix C). This charge controller takes the varying voltage from the PV array and produces a stable 48V voltage for the DC bus. A Single FM-80 controller has output power rating of 3840W and costs $584. Table 5.2 lists the number of controllers required and their corresponding costs.

Table 5.2: MPPT charge controller cost

System KW	MPPT controllers required	Total Cost
1	1	$584
2.5	1	$584
5	2	$1,168
7.5	2	$1,168
10	3	$1,752
20	6	$3,504
30	8	$4,672
40	11	$6,424
50	14	$8,176

5.3 Cost of Energy Storage System(ESS)

The purpose of the proposed off-grid DC micro-grid system for our study area is to supply uninterruptible and maximum quality power to the DC loads in islanded mode. So, to achieve our purpose the cost of every kWh supplied by the ESS is needed. The most important factors to calculate the costs and benefits ESS are the capital cost of the equipment, the cost for recharging energy and the replacements costs if they are needed. The benefits depend on the kind of use required by the user and the expected service of the ESS [59], [60]. The frequency of operation (charge and discharge cycles) is one of the most important parameters to calculate the life-cycle. The applications for ESS can be categorized by whether frequent cycling is expected. This is important because depending on the application, the number of cycles by year will change. For an arbitrage application the ESS will work more than 200 cycles by year. In the other hand, if the ESS is used only for power quality the ESS will work only 20 times by year. In Table 5.3, different operation/use categories are shown [61].

Table 5.3: Operation/Use categories [61]

Category/Definition	Hours of Storage	Use/Duty Cycle	Representative Application
Long-duration storage, frequent discharge	4-8	1 cycle/day x 250 days/year	Load-leveling, Source following, arbitrage
Long-duration storage, infrequent discharge	4-8	20 times/year	Capacity credit
Short-duration storage, frequent discharge	0.25-1	4x15 min cycling x 250 days/year *	Frequency or area regulation
Short-duration storage, infrequent discharge	0.25-1	20 times/year	Power quality, momentary carry-over

*Only able to some technologies (with more than 10000 cycles)

For this study (off-grid DC micro-grid) the economic study is based on the lead-acid batteries with carbon-enhanced electrodes is analyzed for the economical point of view, because it is the latest variation on asymmetric batteries.

- **The capital cost**, can be expressed as:

$$\mathrm{Cost}_{\mathrm{total}}(€) = \mathrm{Cost}_{\mathrm{Pcs}}(€) + \mathrm{Cost}_{\mathrm{ESS}}(€) \tag{5.1}$$

Where

$\mathrm{Cost}_{\mathrm{Pcs}}$: is the cost of the full equipment

$\mathrm{Cost}_{\mathrm{ESS}}$: is the cost of charging the energy.

The cost of the full equipment depends on the power rating of the system:

$$Cost_{Pcs}(€) = UnitCost_{Pcs} * P_{kw} \tag{5.2}$$

For almost all the technologies, the cost of the storage unit depends on the amount of energy stored:

$$Cost_{ESS} = UnitCost_{ESS}\left(\frac{€}{kwh}\right) * E(kwh) \tag{5.3}$$

where E is the stored energy capacity.

All systems have some inefficiency at charging the ESS. To consider these losses, the last equation is modified and expressed as follows:

$$Cost_{ESS} = UnitCost_{ESS}\left(\frac{€}{kwh}\right) * \frac{E(kwh)}{\eta} \tag{5.4}$$

Where η is the round-trip efficiency of the ESS.

As shown, cost is calculated by adding the cost of the storage unit and the cost of the full equipment systems; these are treated separately because they depend on ratings, power and energy [61]. In [61], [62] the cost of the power and energy storage is shown in Table 5.4. These values are used for comparative purpose, because the actual cost of storage systems depends on many factors and hypothesis, therefore the values shown are subjective and continue to be debated even among experts in the field.

Table 5.4. Cost and performance assumptions [61], [62]

Technology	Power Subsystem Cost (€/kW)	Energy Storage Subsystem Cost (€/kWh)	Round-trip Efficiency (%)	Cycles
Advanced Lead-Acid Batteries	315,53	260,31	80	2000
Sodium/sulfur Batteries	276,09	276,09	75	3000
Lead-Acid with Carbon-enhanced electrodes	315,53	260,31	75	20000
Zinc/bromine Batteries	315,53	315,53	70	3000
Vanadium Redox Batteries	315,53	473,30	65	5000
Lithium-ion Batteries	315,53	473,30	85	4000
CAES	552,18	3,94	70	25000
Pumped hydro	946,59	5,916	85	25000
Flywheels	473,30	1262,13	95	25000
Supercapacitors	394,42	7888,30	95	25000

Considering the life-cycle of the batteries same as the total number of cycles that the battery can work, then the price for each kWh generated could be calculated as shown in the following equation.

$$\text{Cost}_{\text{ESS}}\left(\frac{€}{\text{kwh}}\right) = \frac{\text{Cost}_{\text{Pc}}*\text{kw}+\ \text{UnitCost}_{\text{ESS}}*\frac{\text{E(kwh)}}{\eta}}{\text{E}_{\text{kwh}}*\text{cycles}} \qquad (5.5)$$

Using the values shown in the Table 5.4, the cost of each kWh generated for the Lead-acid Batteries will be:

$$\text{Cost}_{\text{ESS}}\left(\frac{€}{\text{kwh}}\right) = \frac{\text{Cost}_{\text{Pc}}*\text{kw}+\ \text{UnitCost}_{\text{ESS}}*\frac{\text{E(kwh)}}{\eta}}{\text{E}_{\text{kwh}}*\text{cycles}} = \frac{315{,}53*68+260{,}31*{}^{68}/_{0.8}}{68*2000} = 0{,}43172\,\frac{€}{\text{kwh}} \qquad (5.6)$$

The Lead-Acid batteries with Carbon-enhanced Electrodes are the energy storage device with more number of cycles, the cost of each kWh generated is:

$$\text{Cost}_{\text{ESS}}\left(\frac{€}{\text{kwh}}\right) = \frac{315{,}53*68+260{,}31*{}^{68}/_{0.75}}{68*2000} = 0{,}06530\,\frac{€}{\text{kwh}} \qquad (5.7)$$

Thus, the lead-acid battery with carbon-enhanced electrodes has been chosen to implement the economical storage management, because the other technologies are not benefitting to be implemented for an optimal participation with the DC distribution network. Table 5.5 shows the calculations for the number of batteries required for a 1kW to 50 kW system and their corresponding costs, assuming two days of autonomy storage is required.:

Table 5.5: Battery bank cost and sizing for 2 days of autonomy storage

2 cloudy Day																		
System	Daily Amp hour			Autonomy capacity Ah			DOD Ah			Paralleled		Series	Total batteries		Battery Kwh capacity		Cost	
Kw	Max (Ah /day)	Min Ah /day	Cloudy days	Max (Ah)	Min (Ah)	DOD	Max (Ah)	Min (Ah)	Battery(Ah)	Max	Min		Max	Min	Max	Min	Max	Min
1	283.33	256.25	2	566.667	512.5	0.8	708.33	640.63	225	3.148	2.847	8	25.2	22.8	27.2	24.6	$3,276	$2,964
2.5	708.3325	640.625	2	1416.6675	1281.25	0.8	1770.825	1601.575	225	7.87	7.1175	8	63	57	68	61.5	$8,190	$7,410

5	1416.665	1281.25	2	2833.335	2562.5	0.8	3541.65	3203.15	225	15.74	14.235	8	126	114	111	323	$16,380	$14,820
7.5	2124.9975	1921.875	2	4250.00	3843.75	0.8	5312.475	4804.725	225	23.61	21.3525	8	191.25	171	204	184.5	$24,570	$22,230
10	2833.33	2562.50	2	5666.67	5125.00	0.8	7083.3	6406.3	225	31.48	28.47	8	252	228	272	246	$32,760.00	$29,640.00
20	5666.67	5125.00	2	11333.33	10250.00	0.8	14166.7	12812.5	225	62.96	56.94	8	504	456	544	492	$65,520.00	$59,280.00
30	8500.00	7687.50	2	17000.00	15375.00	0.8	21259.0	19218.8	225	94.44	85.42	8	756	684	816	738	$98,280.00	$89,920.00
40	11333.33	10250.00	2	22666.67	20500.00	0.8	28333.3	25625.0	225	125.93	113.89	8	1008	912	1088	984	$131,040.00	$118,560.00
50	14166.67	12812.50	2	28333.33	25625.00	0.8	35416.7	32031.3	225	157.41	142.36	8	1260	1139	1360	1230	$163,800.00	$148,070.00

5.4 Distribution Cost

The selection criteria for the distribution conductors is their DC resistance and prices. For the main distribution lines, RH Copper conductor at 10 AWG size is selected based on the ampacity rating, DC resistance, and cost and 18 AWG size is selected to connect a single DC House to the distribution network. Table 5.6 shows the calculated cost for the 2.5 kW. Table 5.7 shows the total distribution cost for the wiring and boost converter (Appendix E) for a 1kW -50 kW system.

Table 5.6: Distribution wiring cost for a 2.5kW system

2.5 KW Wiring Minimum Cost				
		Length(Kft)	Price$/_{kft}$	Cost
RH Copper conductor	1x105	1.2	118.125	$189.64
RH Copper conductor	1/0.AWG	1.34	51.25	$57.0925
			Total	$246.7325

Table 5.7: Distribution wiring and boost converter cost

Distribution Cost		
System Size (KW)	Wiring Cost	Boost Converter Cost
1	$98.693	$140
2.5	$246.7325	$350
5	$493.465	$700
7.5	$740.1975	$1050
10	$986.93	$1,400
20	$1938.34	$2,800
30	$3284.93	$4,200
40	$5100.09	$5,600
50	$6928.00	$7,000

Table 5.8 shows the total cost of DC Distribution System for the DC House. The battery cost is for the best-case scenario, which is only accounting for enough storage for the night-time operations. This cost will multiply if more autonomy storage capacity is desired.

Table 5.8: Total DC system cost

System KW	PV cost	MPPT cost	Battery cost	Distribution		Total DC cost
				Wiring	Boost	
1	$2,868.24	$584	$2,964	$98.693	$140	$6,654.933
2.5	$7,170.60	$584	$7,410	$246.7325	$350	$15,761.3325
5	$14,341.20	$1,168	$14,820	$493.465	$700	$31,522.665
7.5	$21,511.80	$1,168	$22,230	$740.1975	$1050	$46,699.9975
10	$28,682.40	$1,752	$29,640.00	$986.93	$1,400	$62,461.33
20	$56,977.20	$3,504	$59,280.00	$1938.34	$2,800	$124,499.54
30	$85,659.60	$4,672	$89,920.00	$3284.93	$4,200	$187,736.56
40	$113,954.40	$6,424	$118,560.00	$5100.09	$5,600	$249,638.49
50	$142,249.20	$8,176	$148,070.00	$6928.00	$7,000	$312,423.20

5.5 AC System Cost

In order to justify the DC distribution method a comparison study is prepared for the AC distribution cost. The AC system is less efficient because of the extra conversion stages, which are not required in the DC distribution. The AC system requires an inverter to convert DC to AC on the source side. SMA Sunny Boy 10000TLUS-10 2.5kW inverter is selected (Appendix F). The common AC distribution voltage is 15 kV, which means transformers are required to step-up the voltage at the source end and step-down on the house side to supply the house at 220V. The transformer selected for the AC network is ABB Single phase overhead distribution transformer (Appendix G). Table 5.9 details the cost analysis for the AC system. The PV cost for the AC system is calculated assuming system efficiency of 75%. The cost for MPPT charge controller and battery bank remains unchanged from the DC system. But the wiring cost is half of the DC system because smaller cable conductors are needed for the high voltage distribution.

Table 5.9: Total AC system cost

System KW	PV cost	MPPT cost	Battery cost	Inverter Cost	Transformer Cost	Distribution Wiring	Distribution Transformer	Total AC Cost
1	$3,236.46	$584	$2,964	$330.5	$350	$49.346	$500	$8,014.306
2.5	$8,091.15	$584	$7,410	$826.25	$875	$123.366	$1,250	$19,159.766
5	$16,182.30	$1,168	$14,820	$1,652.50	$1,750	$246.73	$2,500	$38,319.53
7.5	$24,273.45	$1,168	$22,230	$2,478.75	$2,625	$370.01	$3,750	$56,895.21
10	$32,558.40	$1,752	$29,640.00	$3,305	$3,500	$493.465	$5,000	$76,248.865
20	$64,729.20	$3,504	$59,280.00	$6,610	$3,250	$969.17	$7,500	$145,842.37
30	$96,900.00	$4,672	$89,920.00	$9,915	$7,000	$1,642.465	$10,000	$220,049.465
40	$129,070.80	$6,424	$118,560.00	$13,220	$8,750	$2,550.045	$12,500	$291,074.845
50	$161,241.60	$8,176	$148,070.00	$16,525	$10,500	$3,464.00	$15,000	$362,976.60

Figure 5.2 graphs the cost difference between the DC and AC distributions. In this Figure 5.2, the DC system is assumed to be at 85% efficiency and AC system to be at 75% efficiency.

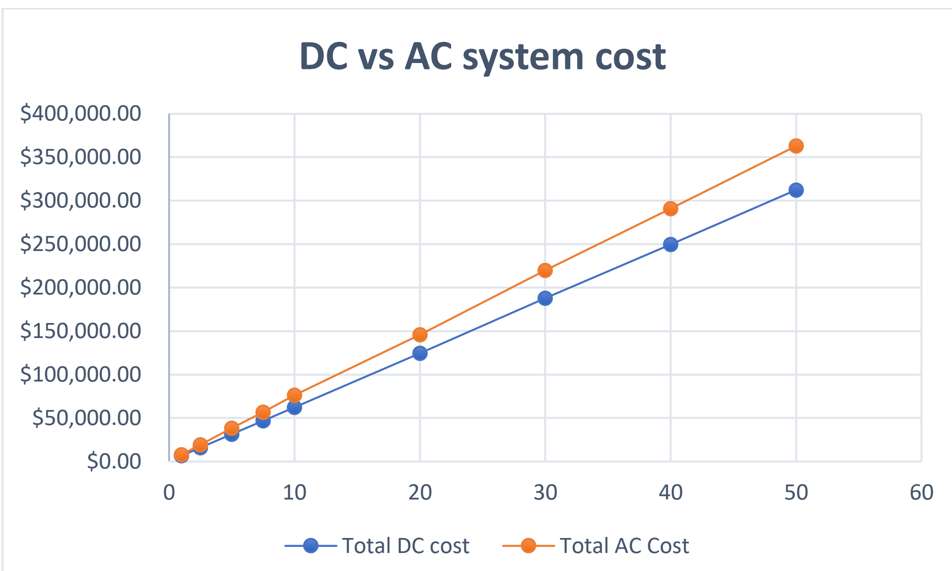

Figure 5.2: DC system cost at 85% efficiency and AC system 75% efficiency

Finally, as shown in Figure 5.2 the cost difference between the two distribution methods grows larger as their efficiency gap increases. Thus, the cost analysis of the designed DC power source with a rating of 2.5 kw of the study area is cost effective and efficient when compared to the AC power source with the same power rating.

Chapter 6

Conclusion and Future Work

6.1: Conclusion

This thesis focuses on the design, modeling, control, simulation, and performance evaluation of an off-grid DC micro-grid distribution system. The complete system was modeled in MATLAB. The simulation results proved that the design meets the DC bus voltage stability requirements under different operating conditions. The PV source is kept at its maximum power generating point by the MPPT controller and the ESS is used to control the voltage level and the power flow through a bidirectional converter, this source will act as a “master” remaining the voltage at 48V and meeting the DC load demand. The distribution network layout was modeled with 5 DC houses. Different kinds of control methods are proposed to increase the injected power, balance the power flow and the voltage level of the off-grid DC micro-grid. The proposed control strategy based on the MPPT control for the PV model and the voltage and power control for the ESS has been implemented in Simulink. The design of the bidirectional converter and the boost converter were done by considering the equivalent circuit and its transfer functions. The control of the boost converter were proven thanks the bode diagrams, root locus, and step response by SISO tool/MATLAB implementation. From the obtained results, the Lead-Acid batteries with enhanced carbon electrodes are optimal to exchange energy with in the off-grid DC micro-grid.

Using the off-grid DC micro-grid developed model in this thesis, off-grid study case was conducted. From the simulation results, various observations were made:

- It is confirmed that PV can work in MPP mode.
- The ESS is able to balance the power flow and stabilize the voltage level.
- Only ESS can work as a “Master” unit to ensure the correct behavior of the system.

Finally, the distribution network layout was modeled with 5 DC houses. The boost converters in the distribution network kept the voltage supplied to the load at 48V. The efficiency of the distribution network depends on the distance that the network has to cover and the conductor type utilized. The losses in the distribution network can be minimized by choosing higher gauge conductors and reducing the distance if possible. This system is at a low voltage distribution which leads to high currents in the network which needs a good protection system. So, the reliable operation of the distribution network is ensured by integrating current interruption devices in case of faults, relays and proper grounding schemes. DC vs. AC cost analysis showed that the off-grid DC micro-grid distribution network is more cost effective of the two systems. The AC distribution is burdened by the extra conversion stages which require extra components and reduce efficiency. Other factors, such as power factor correction and frequency stability, are not relevant in the DC system. The factors together provide for a simple, efficient and cost-effective system.

6.2: Future Work

For simplicity, this study only included PV renewable source as part of the system but the concept of the DC house includes many other renewable sources such as: wind, hydro, human-powered generator. In the future work these sources can also be integrated into a larger simulation model. In the implemented simulations, the sample time was fixed at 1µs (for technical limitations) and the switch frequency at 10kHz (100 µs), so the accuracy not was suitable. For the future, the use of a smaller simple time could give better results. For future work, the implementation of another controller inverter could be interesting, to study the possibilities of the exchange power flow between the grid and the micro-grid system (i.e. ESS). The model could be further validated with pole-to-neutral loads and with the operation of weather dependent units in master mode, as long as provided by a proper control. Future study should also be conducted to determine the most optimum distribution voltage for the DC house system. Overall this thesis produced a basic simulation model for the off-grid DC micro-grid DC house distribution system which will be further built upon in the future.

References

[1] P. Achintya, R. Javier and e. al, "Design and Verification of Smart and Scalable DC Microgrid for emerging regions," University of California, USA, 2012.

[2] H. S. Bassi, "Design and Modeling of Centralized Distribution," © 2013, the Faculty of California Polytechnic State University,, 2013.

[3] Evan Lim and Samson Liu, "Wind Power Generator Design," © 2011 Evan Lim and Samson Liu, the Faculty of the Electrical Engineering Department California Polytechnic State University, San Luis Obispo , 2011.

[4] O. Jong, "Multiple Input Single Output (MISO) DC-DC Converter," California Polytechnic University, San Luis Obispo, 2012.

[5] UNEC, "Energy Access and Securty in Eastern Africa:Status and Enhancement Pathways," United Nations Economic Commission for Africa, Addis Ababa, 2014.

[6] Rehma and S. L., "Energy for sustainabledevelopment in Indea:linkages and strategic direction," energy police, vol. 34, no. 5, pp. 643-654, march 2006.

[7] D. m. a. n. n. b. t. sector, "enthernet," february 2014. [Online]. Available: http://greentechleadership.org/dc-microgri-nanogrid-next-big-thing-energy-sector. [Accessed 16 may 2014].

[8] group WPS4-1054, " Intelligent Control for Distibuted System," 47th International Universities', Denmark, 2012.

[9] Peng Wang,Xiong Liu,Chi ,JinPohchiang Loh,Fookhoong Choo, "A Hybrid AC/DC Micro-Grid," ©2011 IEEE, Singapore, 2011.

[10] N. Zhi, "Power Control of DC Microgrid With Variable generation and energy storage," International Journal of Automation and Power Engineering (IJAPE), vol. 2, no. 4, pp. 252-256, May 2013.

[11] L. Priyadarshanee, "modeling and control of hybride AC-DC micro grid, MSC thesis," ODISHA: nationa institute of technology, 2012.

[12] D. SALOMONSSON, "Modeling, Control and Protection of Low-Voltage DC Microgrid," Stockholm: Royal Institute of T echnology, Stockholm, 2008.

[13] E.r.p.p.o.t.population,"Ethiopiapopulation.org,"2017.[Online].Available: http://Ethiopiapupulation.org/Ethiopia rural pupulation percentage. [Accessed 16 10 2017].

[14] L. Roggia, L. schuch and e. al, "design of a sustainable residential microgrid system with DC and AC buses including PHEV and energy storage," International Conference on Renewable Energies and Power Quality, Canaria, spain, april 2010.

[15] N.R. Rahmanov,N.M. Tabatabaei,K. Dursun,O.Z. Kerimov, "COMBINED AC-DC MICROGRIDS," IJTPE, vol. 4, no. 12, pp. 158-161, 2012 .

[16] D Ravi Prasad, Dr B.Rajesh Kamath, K.R Jagadisha, S.K Girish, "Smart DC Micro-grid for Effective Utilization of," International Journal of Scientific & Engineering Research, vol. 3, no. 12, pp. 1-5, December-2012.

[17] B. M. M. Mwinyiwiwa, "DC Bus Voltage Regulator for Renewable Energy," International Journal of Electrical, Computer, Energetic, Electronic and Communication Engineering, vol. 7, no. 12, pp. 1629-1633, 2013.

[18] Kim, S. K., J. H. Jeon, C. H. Cho, and E. S. Kim,, "Modeling and simulation of a grid-connected PV generation system for electromagnetic transient analysis," in Solar Energy, vol. 83, pp. 664-678,, May 2009.

[19] H. L. Tsai, "Insolation-oriented model of photovoltaic module using Matlab/Simulink," in Solar Energy, vol. 84, pp. 1318-1326, July 2010..

[20] Femia, N., G. Petrone, G. Spagnuolo and M. Vitelli, "Optimizing sampling rate of P&OMPPT technique," in Proceedings of the IEEE 35 Annual Power Electronics Specialists conference, June 2004.

[21] Tariq, A., and M. S. J. Asghar,, "Development of microcontroller-based maximum power point tracker for a photovoltaic panel," in Proceedings of the IEEE Power India Conference, 2006.

[22] Sofla, M. A., and Lingfeng Wang., "Control of DC-DC bidirectional converters for interfacing batteries in microgrids," in Power Systems Conference and Exposition (PSCE), 2011 IEEE/PES, March 2011.

[23] Wei, L. Joos, G., and C. Abbey, "A Parallel Bidirectional DC/DC Converter Topology for Energy Storage Systems in Wind Applications," in Industry Applications Conference, 2007. 42nd IAS Annual Meeting. Conference Record of the 2007 IEEE, Sep. 2007.

[24] Ramprabhakar, J., and K. Ragavan, "Dual bi-directional converter control for wind-solar-hydro system in grid connected and islanded operation," in Power Electronics, Drives and Energy Systems (PEDES), 2012 IEEE International Conference, Dec.2012.

[25] Fenil V Gadhethariya ,Melvin Z. Thomas, "Analysis of Voltage Droop Control of Dc Micro-Grid," Indian Journal of Applied Science, vol. 4, no. 5, pp. 235-238, May 2014.

[26] W. Leslau, Zway Ethiopic Documents: Grammar and Dictionary. Wiesbaden, Otto Harrassowitz. p. xv. ISBN 3447041625, 1996.

[27] Robert Mepham, R. H. Hughes, and J. S. Hughes,, "A Directory of African Wet Lands," Cambridge, Cambridge: IUCN, UNEP and WCMC, 1992, p. 158.

[28] Water Resources and Irrigation Development in Ethiopia - IWMI, "Table 3. Basic hydrological data of lakes and reservoirs of Ethiopia," 18 july 2011. [Online]. Available: 2011 at the Wayback Machine. [Accessed 2 july 2011].

[29] "Google Earth," [Online].

[30] N. S, “Climate, "Table A.2. Central Statistical Agency website," 13 November 2010. [Online]. Available: Wayback Machine. [Accessed 26 December 2009].

[31] H. Weld Blundell, "Exploration in the Abai Basin, Abyssinia," The Geographical Journal, pp. 529-551, 1906.

[32] "Information on Fisheries Management in the Federal Democratic Republic of Ethiopia," report dated January, 2003.

[33] A. Circuits, "Skin Effect," [Online]. Available," 2013. [Online]. Available: http://www.allaboutcircuits.com/vol_2/chpt_3/6.html. [Accessed 2013].

[34] J.Parmar,"What is Corona Effect [Online]. Available," 23 March 2011. [Online]. Available: http://electricalnotes.wordpress.com/2011/03/23/what-is-corona-effect.

[35] Taufik, "The DC House Project Promoting Sustainable Innovations in Renewable Energy Technology," California Polytechnic State University, San Luis Obispo.

[36] Gab-Su Seo; Jongbok Baek; Kyusik Choi; Hyunsu Bae; Bohyung Cho, "Modeling and analysis of DC distribution systems," in Power Electronics and ECCE Asia (ICPE & ECCE), 2011 IEEE 8th International Conference , 2011.

[37] J. Kuderna, "RV Basics: 12-Volt DC Systems," RVtravel, [Online]. Available:," [Online]. Available: http://rvtravel.com/publish/12volt_DC_systems.shtml. [Accessed 2013].

[38] Pratt, A.; Kumar, P.; Aldridge, T.V,"Evaluation of 400V DC distribution in telco and data centers to improve energy efficiency" in Telecommunications Energy Conference, 2007. INTELEC 2007. 29th International , 2007.

[39] B. G. F. Sandeep Anand, "Optimal voltage level for DC microgrids," in IECON 2010 - 36th Annual Conference on IEEE Industrial Electronics Society, U.S.A, 2010.

[40] J.Pellis., "The DC low-voltage house. Graduation project," Eindhoven University of Technology, 1997.

[41] B. J. Williamson, "project Edison: Smart DC," ISGT Europe 2011, pp. 1-10, December 2011.

[42] X. M. Y. Z. a. c. m. Weixing Li, "On voltage standards for DC home microgrids energized by distributed sources," in Power Electronics and Motion Control Conference, 2012.

[43] B. G. F. Sandeep Anand, "Optimal voltage level for DC microgrids," IECON 2010-36th Annual Conference on IEEE Industrial Electronics Society, pp. 3034-3039, 2010.

[44] J. M. Guerrero, J. C. Vasquez, J. Matas, L. G. de Vicuna, and M. Castilla, "Hierarchical control of droop-controlled AC and DC microgrids—a general approach toward standardization," Industrial Electronics, IEEE Transactions *on*, vol. 58, no. 1, p. 158–172, 2011.

[45] Grégoire Léna (IED), "Rural Electrification with PV Hybrid Systems Overview and Recommendations for Further Deployment," IEA International Energy Agency, July 2013 .

[46] Phang, J.C.H., Chan, D.S.H., & Philips, J.R.,, "Accurate Analytical Method for the Extraction of Solar Cell Model Parameter," IEEE Electronics Letters, vol. 20, no. 10, pp. 406-408, 1984.

[47] Marcelo Gradella Villalva, Jonas Rafael Gazoli, and Ernesto Ruppert Filho, "Comprehensive Approach to Modeling and Simulation of Photovoltaic Arrays," IEEE TRANSACTIONS ON POWER ELECTRONICS, vol. 24, no. 5, pp. 1198-1199, MAY 2009.

[48] Aeronautics and Space Administration, Solar Cell Array Design Handbook, et Pro-pulsion Lab,, 1976.

[49] K.H.Hussein; I.Muta;T.Hoshino; M.Osakada, "Maximum photovoltaic power tracking: an algorithm for rapidly changing atmospheric conditions," IEE Proceedings - Generation, Transmission and Distribution, vol. 142, no. 1, pp. 59-64, Jan 1995.

[50] R. W. Erickson, Fundamentals of Power Electronics, University of Colorado, Boulder: 912 pages, 1997.

[51] N. MOHAN, POWER ELECTRONICS Converters,Applications, and Design, Minneapolis, Minnesota: John Wiley and Sons, Inc., 1995.

[52] M. Swierczynski, R. Teodorescu, C. N. Rasmussen, P. Rodriguez, and H.Vikelgaard, "Overview of the energy storage systems for wind power integration enhancement," Industrial Electronics (ISIE), p. 3749–3756, 2010 IEEE International Symposium on.

[53] Kyohei Kurohane, Akie Uehara, Tomnonobu Senjya, Atsushi Yona, NaomitsuUrasaki, Toshihisa Funabashi, and Chul-Hwan Kim,, "Control strategy for a distributed DC power system with renewable energy," vol. 36, p. 42–49, 2011.

[54] M. Rivera, "Small Wind / Photovoltaic Hybrid Renewable Energy System Optimization, MSc Thesis," University of Puerto Rico., Puerto Rico, 2008.

[55] Sandia National Laboratories, Standalone Photovoltaic Systems: a Handbook of Recommended Design Practices, New Mexico: Daystar, Inc. Las Cruces, 1995.

[56] Haque ME, Muttaqi KM, Negnevitsky M, "Control of a standalone variable speed wind turbine with apermanent magnet synchronous generator," in in the Proceedings of the IEEE Power and Energy SocietyGeneral Meeting—Conversion and Delivery of Electrical Energy in the 21st Century, 2008.

[57] Hu X, Xiong R, Egardt B., "Model-based dynamic power assessment of lithium-ion batteries considering different operating conditions," in Industrial Informatics, IEEE Transactions on, 10(3), 2014.

[58] J. E. Chaidez, "DC House Modeling and System Design," California Polytechnic State University, San Luis Obispo, June 2011.

[59] S. M. Schoenung and J. Eyer, "Benefit/Cost Framework for Evaluating Modular Energy Storage".

[60] J. M. Eyer, J. J. Iannucci, and G. P. Corey, Energy Storage Benefits and Market Analysis Handbook A Study for the DOE Energy Storage Systems Program, Sandia: Sandia National Labratories, 2004.

[61] S. M. Schoenung, "Energy Storage Systems Cost Update," in Energy Storage Systems Cost Update, SAND, 2011, pp. SAND2011-2730.

[62] A. Price, G. Thijssen, and P. Symons, "Electricity Storage, A Solution in Network Operation," Distributech Europe, 2000.

Appendices

A. Implemented off-grid DC micro-grid in Simulink

B. BP Solar SX3190W solar module data sheet

C. FLEXmax continuous MPPT controller's datasheet

D. Lead acid battery with carbon enhanced electrode data sheet

E. Boost converter for the distribution network and battery bank specifications

F. SMA SUNNY BOY 10000TL-US inverter datasheet

G. ABB single phase overhead distribution transformer

H. proportional and integral terms

Appendix A

Implemented off-grid DC micro-grid in Simulink

1. PV model:

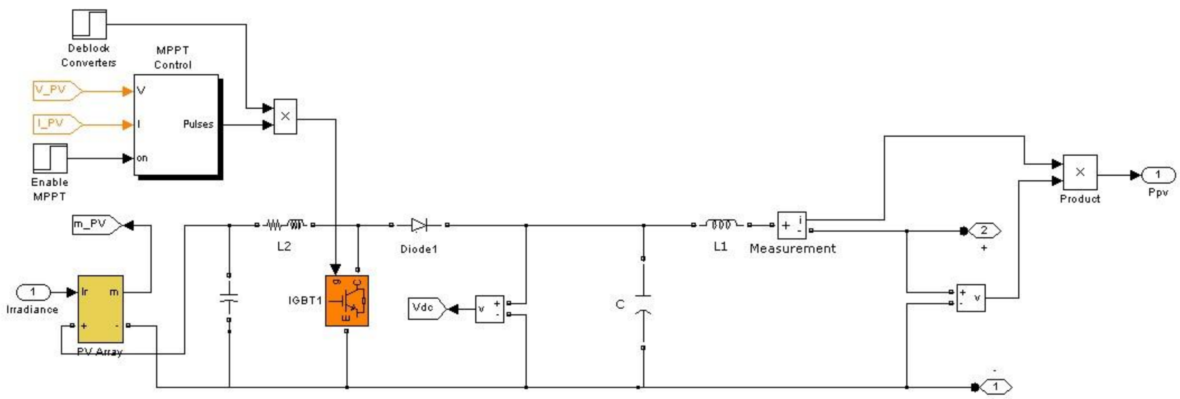

1.1 PV Array:

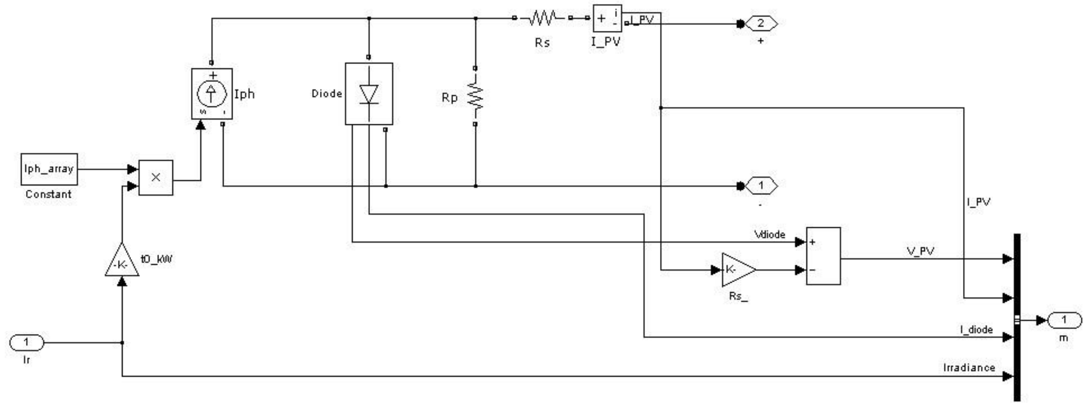

1.2 MPPT Control:

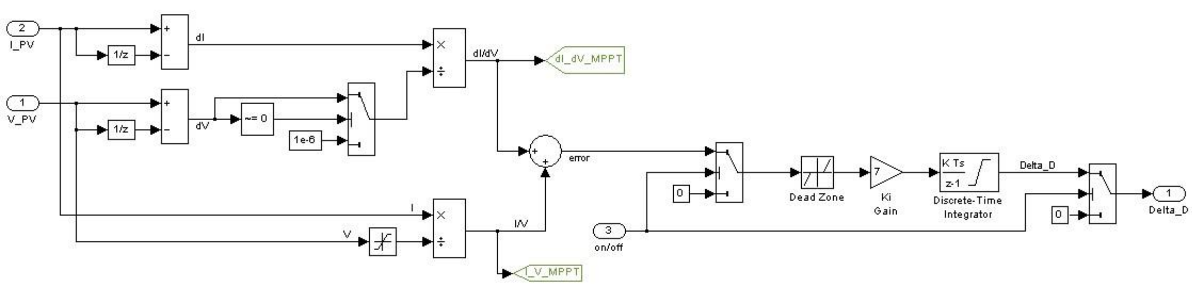

2. ESS model:

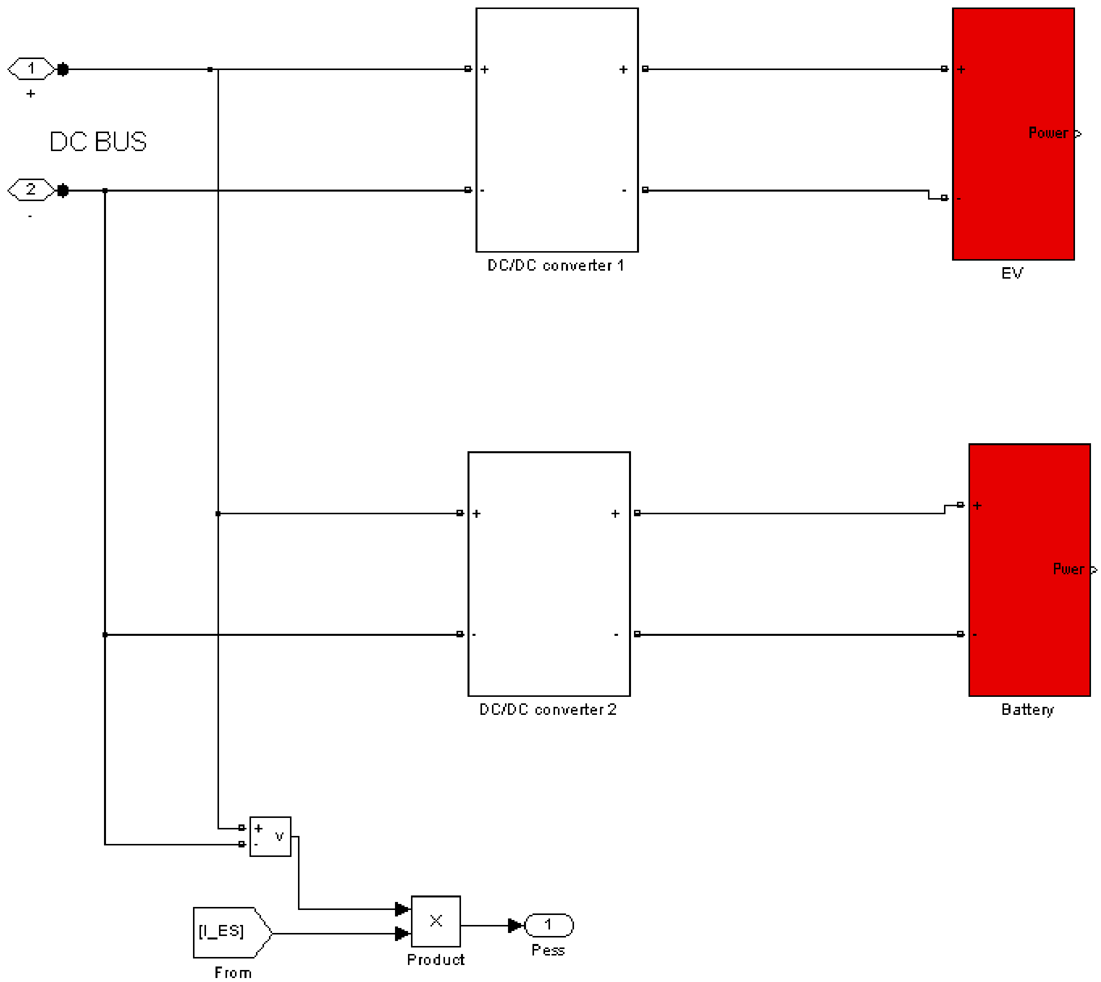

2.1 Battery model:

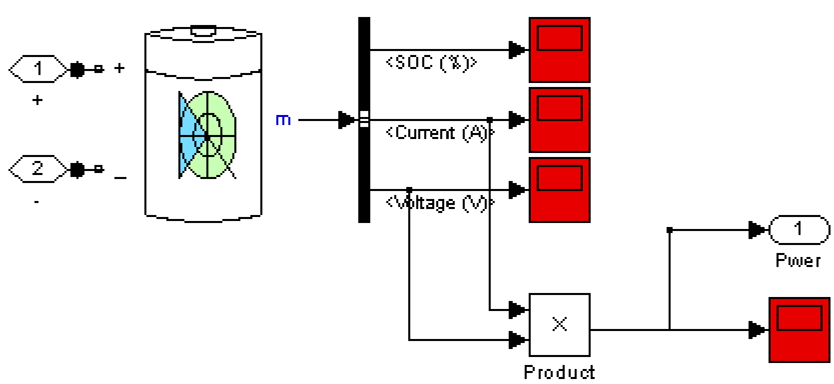

2.2 Bi-directional Converter:

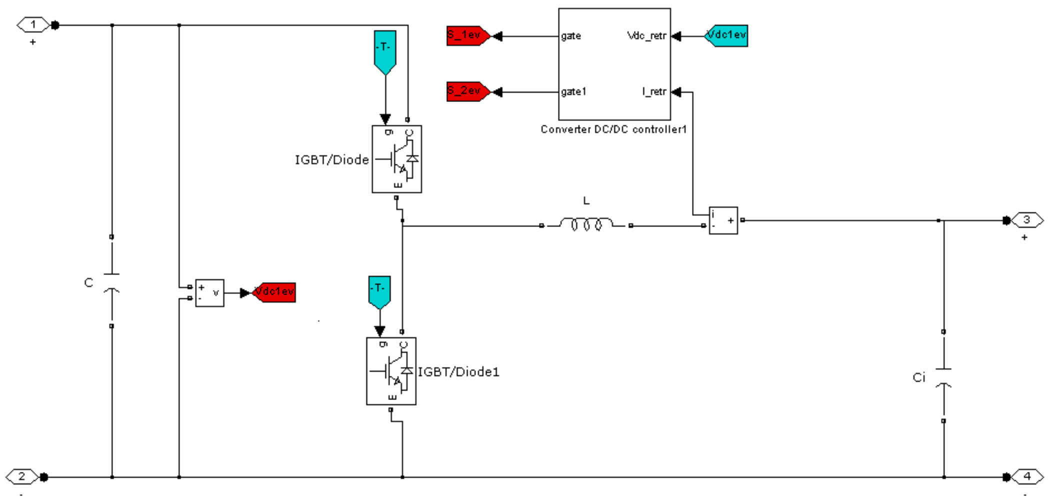

2.3 Bi-directional Control:

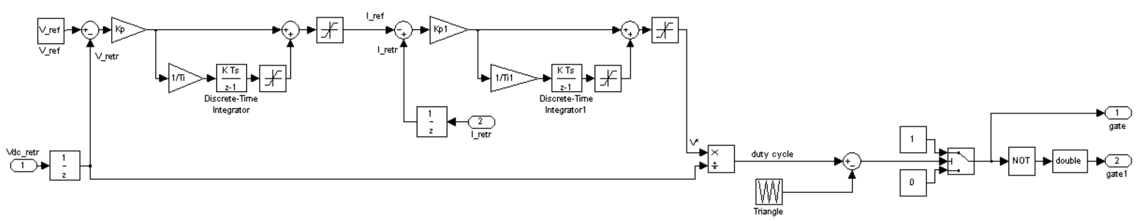

Appendix B

BP Solar SX3190W solar module data sheet

bp solar

SX 3195

195 watt photovoltaic module

High-efficiency photovoltaic module using silicon nitride multicrystalline silicon cells

Performance

Rated power (P_{max})	195W
Power tolerance	±9%
Nominal voltage	16V
Limited Warranty[1]	25 years

Configuration

S Silver frame with output cables and polarized Multicontact (MC) connectors

B Bronze frame with output cables and polarized Multicontact (MC) connectors

Electrical Characteristics[2]	SX 3195	SX3190
Maximum power (P_{max})[3]	195W	190W
Voltage at P_{max} (V_{mp})	24.4	24.3V
Current at P_{max} (I_{mp})	7.96A	7.82A
Warranted minimum P_{max}	177.5W	172.9W
Short-circuit current (I_{sc})	8.6A	8.5A
Open-circuit voltage (V_{oc})	30.7V	30.6V
Temperature coefficient of I_{sc}	(0.065±0.015)%/°C	
Temperature coefficient of V_{oc}	-(111±10)mV/°C	
Temperature coefficient of power	-(0.5±0.05)%/°C	
NOCT (Air 20°C; Sun 0.8kW/m²; wind 1m/s)	47±2°C	
Maximum series fuse rating	15A	
Maximum system voltage	600V (U.S. NEC rating)	

Mechanical Characteristics

Dimensions	Length: 1680mm (66.14") Width: 837mm (32.95") Depth: 50mm (1.97")
Weight	15.4 kg (33.95 pounds)
Solar Cells	50 cells (156mm x 156mm) in a 5x10 matrix connected in series
Output Cables	RHW-2 AWG# 12 (4mm²), cable with polarized weatherproof DC rated Multicontact connectors; asymmetrical lengths - 1250mm (-) and 800mm (+)
Diodes	***IntegraBus™*** technology includes Schottky by-pass diodes integrated into the printed circuit board bus
Construction	Front: High-transmission 3mm (1/8th in) tempered glass; Back: Tedlar; Encapsulant: EVA
Frame	**S** Anodized aluminium alloy type 6063T6 Universal frame; Color: silver **B** Anodized aluminium alloy type 6063T6 Universal frame; Colour: bronze

1. Module warranty: 25-year limited warra[illegible] limitec warranty of materials and workmanship. See your local representative for full terms of these warranties.
2. This data represents the performance of typical SX 3195 products, and is based on measurements made in accordance with ASTM E1036 correctec to SRC (STC.)
3. During the stabilization process that occurs during the first few months of deployment, module power may decrease by up to 1% from typical P_{max}.

 6802.0013 REV 1 06/07

Quality and Safety

ESTI	Module power measurements calibrated to World Radiometric Reference through ESTI (European Solar Test Installation at Ispra, Italy)
®	Listed by Underwriter's Laboratories for electrical and fire safety (Class C fire rating)

SX 3195 I-V Curves

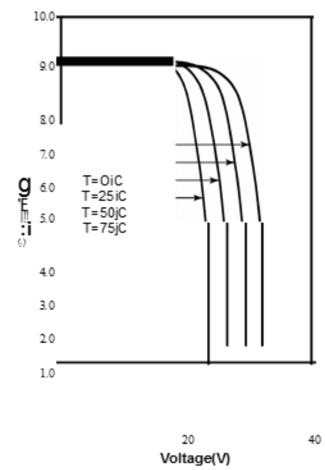

Qualification Test Parameters

Temperature cycling range	-40°C to +85°C (-40°F to 185°F)
Humidity freeze, damp heat	85% RH
Static load front and back (e.g. wind)	2,400 pa (50psf)
Front loading (e.g. snow)	5,400 pa (113psf)
Hailstone impact	25mm 0 (1 inch) at 23 m/s (52mph)

Module Diagram

Dimensions in brackets are in inches. Un-bracketed dimensions are in millimeters. Overall tolerances ±3mm (1/8").

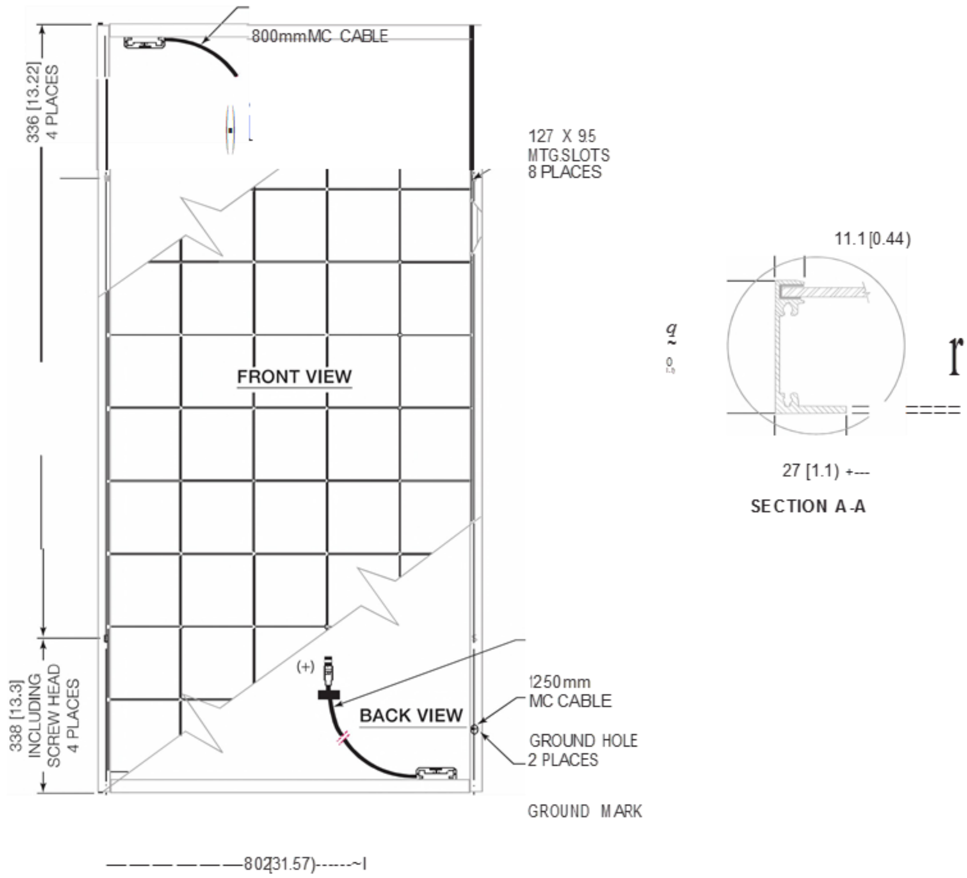

Included with each module: self-tapping grounding screw, instruction sheet and warranty documents.

Note: This publication summarizes product warranty and specifications, which are subject to change without notice. Additional information may be found on our web site: **www.bpsolar.us**

Appendix C

FLEXmax Continuous MPPT Controllers Datasheet


FLEXmax

Continuous Maximum Power Point Tracking Charge Controllers

- Increases PV Array Output by up to 30%
- Advanced Continuous Maximum Power Point Tracking
- Full Power Output in Ambient Temperatures up to 104°F (40°C)
- Battery Voltages from 12 VDC to 60 VDC
- Fully OutBack Network Integrated and Programmable
- Programmable Auxiliary Control Output
- Built-in 128 days of Data Logging
- Standard 5 Year Warranty

The FLEXmax family of charge controllers is the latest innovation in Maximum Power Point Tracking (MPPT) charge controllers from OutBack Power Systems. The innovative FLEXmax MPPT software algorithm is both continuous and active, increasing your photovoltaic array power yield up to 30% compared to non-MPPT controllers. Thanks to active cooling and intelligent thermal management cooling, both FLEXmax charge controllers can operate at their full maximum current rating, 60 Amps or 80 Amps respectively, in ambient temperatures as high as 104°F (40°C).

Included in all of the FLEXmax Charge Controllers are the revolutionary features first developed by OutBack Power, including support for a wide range of nominal battery voltages and the ability to step-down a higher voltage solar array to recharge a lower voltage battery bank. A built-in, backlit 80 character display shows the current status and logged system performance data for the last 128 days at the touch of a button. The integrated OutBack network communications allows FLEXmax series Charge Controllers to be remotely programmed and monitored via a MATE system display and provides unrivaled complete system integration.

FLEXmax MPPT Charge Controllers are the only choice when you demand a high performance, efficient and versatile charge controller for your advanced power system.

OutBack Power Systems

www.outbackpower.com

Figure C-1: FLEXmax Continuous MPPT Controllers Datasheet Page 1

FLEXmax Specifications

	FLEXmax 80 - FM80-150VDC	FLEXmax 60 - FM60-150VDC
Nominal Battery Voltages	12, 24, 36, 48, or 60 VDC (Single model - selectable via field programming at start-up)	12, 24, 36, 48, or 60 VDC (Single model - selectable via field programming at start-up)
Maximum Output Current	80 amps @ 104° F (40°C) with adjustable current limit	60 amps @ 104° F (40°C) with adjustable current limit
Maximum Solar Array STC Nameplate	12 VDC systems 1250 Watts / 24 VDC systems 2500 Watts / 48 VDC systems 5000 Watts / 60 VDC Systems 7500 Watts	12 VDC systems 900 Watts / 24 VDC systems 1800 Watts / 48 VDC systems 3600 Watts / 60 VDC Systems 4500 Watts
NEC Recommended Solar Array STC Nameplate	12 VDC systems 1000 Watts / 24 VDC systems 2000 Watts / 48 VDC systems 4000 Watts / 60 VDC Systems 5000 Watts	12 VDC systems 750 Watts / 24 VDC systems 1500 Watts / 48 VDC systems 3000 Watts / 60 VDC Systems 3750 Watts
PV Open Circuit Voltage (VOC)	150 VDC absolute maximum coldest conditions / 145 VDC start-up and operating maximum	150 VDC absolute maximum coldest conditions / 145 VDC start-up and operating maximum
Standby Power Consumption	Less than 1 Watt typical	Less than 1 Watt typical
Power Conversion Efficiency	97.5% @ 80 Amps in a 48 VDC System - Typical	98.1% @ 60 Amps in at 48 VDC System voltage - Typical
Charging Regulation	Five Stages: Bulk, Absorption, Float, Silent and Equalization	Five Stages: Bulk, Absorption, Float, Silent and Equalization
Voltage Regulation Setpoints	10 to 60 VDC user adjustable with password protection	10 to 60 VDC user adjustable with password protection
Equalization Charging	Programmable Voltage Setpoint and Duration - Automatic Termination when completed	Programmable Voltage Setpoint and Duration - Automatic Termination when completed
Battery Temperature Compensation	Automatic with optional RTS installed / 5.0 mV per °C per 2V battery cell	Automatic with optional RTS installed / 5.0 mV per °C per 2V battery cell
Voltage Step-Down Capability	Can charge a lower voltage battery from a higher voltage PV array - Max 150 VDC input	Can charge a lower voltage battery from a higher voltage PV array - Max 150 VDC input
Programmable Auxilary Control Output	12 VDC output signal which can be programmed for different control applications (Maximum of 0.2 amps DC)	12 VDC output signal which can be programmed for different control applications (Maximum of 0.2 amps DC)
Status Display	3.1" (8 cm) backlit LCD screen - 4 lines with 80 alphanumeric characters total	3.1" (8 cm) backlit LCD screen - 4 lines with 80 alphanumeric characters total
Remote Display and Controller	Optional Mate or Mate2 with RS232 Serial Communications Port	Optional Mate or Mate2 with RS232 Serial Communications Port
Network Cabeling	Proprietary network system using RJ 45 Modular Connectors with CAT 5e Cable (8 wires)	Proprietary network system using RJ 45 Modular Connectors with CAT 5e Cable (8 wires)
Data Logging	Last 128 days of Operation - Amp Hours, Watt Hours, Time in Float, Peak Watts, Amps, Solar Array Voltage, Max Battery Voltage Min Battery Voltage and Absorb for each day along with total Accumulated Amp Hours, and kW Hours of production	Last 128 days of Operation - Amp Hours, Watt Hours, Time in Float, Peak Watts, Amps, Solar Array Voltage, Max Battery Voltage Min Battery Voltage and Absorb for each day along with total Accumulated Amp Hours, and kW Hours of production
Hydro Turbine Applications	Consult factory for approved Turbines	Consult factory for approved Turbines
Positive Ground Applications	Requires two Pole Breakers for switching both positive and Negative Conductors on both Solar Array and Battery Connections (HUB 4 and HUB 10 can not be used for use in positive ground applications)	Requires two Pole Breakers for switching both positive and Negative Conductors on both Solar Array and Battery Connections (HUB 4 and HUB 10 can not be used for use in positive ground applications)
Operating Temperature Range	Minimum -40° to maximum 60° C (Power capacity of the controller is automatically derated when operated above 40° C)	Minimum -40° to maximum 60° C (Power capacity of the controller is automatically derated when operated above 40° C)
Environmental Rating	Indoor Type 1	Indoor Type 1
Conduit Knockouts	One 1" (35mm) on the back; One 1" (35mm) on the left side; Two 1" (35mm) on the bottom	One 1" (35mm) on the back; One 1" (35mm) on the left side; Two 1" (35mm) on the bottom
Warranty	Standard 5 year / Available 10 Year	Standard 5 year / Available 10 Year
Weight - Unit	12.20 lbs (5.56 kg)	11.65 lbs (5.3 kg)
- Shipping	15.75 lbs (7.10 kg)	14.55 lbs (6.4 kg)
Dimensions - Unit	16.25" x 5.75" x 4" (41.3 x 14 x 10 cm) - (H x W x D)	13.5 x 5.75 x 4" (40 x 14 x 10 cm)
- Shipping	21" x 10.5" x 9.75" (53 x 27 x 25 cm)	18 x 11 x 8" (46 x 30 x 20 cm)
Options	Remote Temperature Sensor (RTS), HUB 4, HUB 10, MATE, MATE 2	Remote Temperature Sensor (RTS), HUB 4, HUB 10, MATE, MATE 2
Menu Languages	English & Spanish	English & Spanish

OutBack Power Systems™

Main Office:
19009 62nd Avenue NE
Arlington, WA 98223 USA
Phone: (360) 435.6030
Fax: (360) 435.6019

European Office:
C/ Castelló, 17
08830 - Sant Boi de Llobregat
BARCELONA, España
Phone: +34.93.654.9568

www.outbackpower.com

Available From:

7/02/08

Figure C-2: FLEXmax Continuous MPPT Controllers Datasheet Page 2

Appendix D

Lead acid battery with carbon enhanced electrode data sheet

Carbon-Enhanced Lead-Acid Batteries

Improving the performance and reducing the cost of lead-acid batteries for large-scale energy storage

U.S. DEPARTMENT OF ENERGY | Electricity Delivery & Energy Reliability
Energy Storage Program
Sandia National Laboratories

Lead-acid batteries are currently used in a variety of applications, ranging from automotive starting batteries to storage for renewable energy sources.

Lead-acid batteries form deposits on the negative electrodes that hinder their performance, which is a major hurdle to the wider use of lead-acid batteries for grid-scale energy storage. The formation of deposits is exacerbated under the operating conditions required by many large-scale energy storage systems, which cycle at a high electrical current while remaining in a partially charged state (high-rate, partial state of charge operation, or HRPSoC).

In 1997, researchers made two important advancements to lead-acid batteries. First, the Japan Storage Battery Company showed that adding carbon to the battery dramatically reduces the formation of deposits, thereby increasing performance and lifetime. However, the mechanism by which certain carbons enhance battery performance remains unclear. Second, the Australian Commonwealth Scientific and Industrial Research Organization developed the UltraBattery®, which combines a lead-acid battery and a capacitor into a single cell, with the capacitor acting as a buffer of the high rates of charge/discharge. The UltraBattery® allows the battery to be used for long periods in HRPSoC. This reduces the stress on the lead-acid battery, allowing a much longer life, as well as a quick charge acceptance and power discharge.

Technology Benefits

Sealed Lead-Acid Batteries

- Eliminate the threat of an acid spill or emissions and require little maintenance, due to the battery's sealed design
- Exhibit low self-discharge

Carbon-Enhanced Lead-Acid Batteries

- Improve battery cycle life dramatically
- Require minimal modification of existing industrial-scale manufacturing processes
- Offer a potential low-cost, high-performance energy storage solution for grid-scale applications

Overview

The Office of Electricity Delivery and Energy Reliability's Energy Storage Systems (ESS) Program is funding research and testing to improve the performance and reduce the cost of lead-acid batteries. Research to understand and quantify the mechanisms responsible for the beneficial effect of carbon additions will help demonstrate the near-term feasibility of grid-scale energy storage with lead-acid batteries, and may also benefit other battery chemistries.

The ESS Program is also working with Ecoult on its UltraBattery® technology to characterize and measure its performance in various applications. In addition, the solar smoothing functionality of the UltraBattery® technology is being demonstrated in a 500 kWh solar energy smoothing and 1 MWh solar energy shifting demonstration project with the Public Service Company of New Mexico (PNM).

Technology Breakthrough

Above left: Adding carbon to a lead-acid battery improves its performance and lifetime compared to conventional technology.

Above right: The Public Service Company of New Mexico (PNM) grid-scale demonstration project.

Below: The PNM grid-scale demonstration project shows that the UltraBattery® can smooth the variable output of the solar panels.

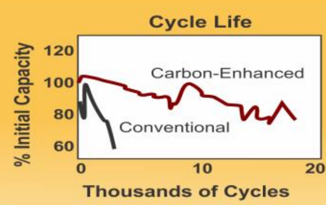

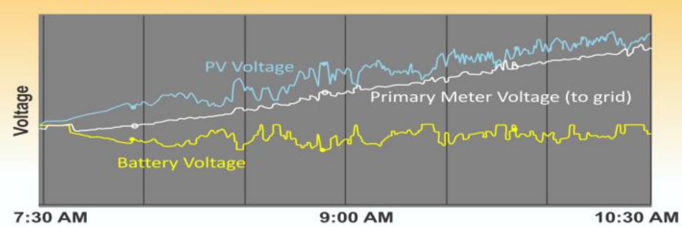

Project Timeline

Ongoing research and development will reduce the costs and improve the performance of lead-acid batteries.

1997:
Research shows that adding carbon to a lead-acid battery greatly reduces the accumulation of a deposit within the battery, increasing the battery performance and lifetime.

Dr. Lam Lan develops the UltraBattery®, a lead-acid battery that uses a capacitor to buffer high rates of charge.

2002:
Different carbon forms are shown to offer very different benefits for battery performance and lifetime.

2006:
The Advanced Lead Acid Battery Consortium initiates the carbon-enhanced lead-acid battery demonstration project.

2007: East Penn Manufacturing becomes licensee of UltraBattery® for global markets outside Japan and Thailand.

2009:

East Penn Manufacturing receives several U.S. Department of Energy grants to pursue advanced lead-acid battery research.

2010:
August: Sandia National Laboratories (SNL) enters a Cooperative Research and Development Agreement (CRADA) with East Penn Manufacturing to study the effect of carbon on lead-acid batteries.

2011:
October: The PNM grid-scale demonstration is commissioned using the UltraBattery® for smoothing and advanced lead carbon for shifting. This project has already proven the solar smoothing functionality of the UltraBattery® technology.

2012:
June: The PJM grid-scale demonstration (3 MW) is commissioned using the UltraBattery®.

December: The SNL/East Penn Manufacturing CRADA project will end. Electrochemical characterization and cycling results from batteries using several types of carbon will be compared with chemical and structural analysis of the carbons and carbon-enhanced anodes. The findings will be used to evaluate the effect of cycling on the batteries.

Challenges

- Sulfate deposits accumulate on the electrode surface, limiting the capacity and cycle life of lead-acid batteries
- Researchers do not yet fully understand the characteristics of carbon that are beneficial or detrimental to lead-acid batteries
- Lead-acid batteries have a low energy-to-weight ratio compared to other battery types
- Lead-acid batteries are slower to recharge than other battery types

Project Partners

- Sandia National Laboratories
  www.sandia.gov
- East Penn Manufacturing
  www.dekabatteries.com
- Ecoult
  www.ecoult.com

Appendix E

Boost converter for the distribution network and battery bank specifications

500W 600W 10A 10~60V to 12~80V DC-DC Switching Boost Converter Power Supply DIY
by BlueSolar
Be the first to review this item

Available from these sellers.

1 new from $28.10

Share

Product Description

Specification:

Module Properties: Step-up / Boost DC-DC Converter

Input Voltage: DC 10 ~ 60 V

Output Voltage: DC 12 ~ 80 V (adjustable, O/p Voltage > I/p Voltage by 2V)

Output Current: 10A Max

Input Current: 15 A Max(Under normal circumstances please 12A Current)

The minimum voltage difference: 2V

Output Power: input 12V Max 120W, in 24V Max 240W, in 60V Max 600W (P=U * I)

Efficiency: 95% Max (eg input :30V output: 40V 5A n: 93%)

Output Short-circuit Protection : yes

Input Reverse Protection: None

Size: 85 x 63 x 64 mm (L*W*H)

Weight: 250g

Figure E-1: Boost Converter for the Distribution network and Battery Bank description

Appendix F

SMA SUNNY BOY 10000TL-US Inverter Datasheet


SMA

SUNNY BOY 8000TL-US / 9000TL-US / 10000TL-US

SB 8000TLUS-10 / SB 9000TLUS-10 / SB 10000TLUS-10

TRANSFORMERLESS TECHNOLOGY

Efficient
- Maximum efficiency of 98.3%
- Transformerless, with H5 topology

High Yields
- Superior yield with OptiTrac MPP tracking
- OptiCool™ active temperature management

Safe
- SMA Power Balancer for three-phase grid connection
- Integrated DC load disconnect and combiner box
- UL 1741/IEEE-1547 compliant

SUNNY BOY 8000TL-US / 9000TL-US / 10000TL-US

Transformerless design, maximum yields

The new Sunny Boy TL-US series is UL-listed for North America and features SMA's innovative H5 topology, resulting in superior efficiencies of up to 98 percent and unmatched solar yields. The transformerless design reduces weight, increases the speed of payback and provides optimum value for any decentralized, commercial PV system. The Sunny Boy TL-US series for North America is the ideal choice for mid-size and large plants from 24 kWp up to the megawatt range.

Figure F-1: SMA SUNNY BOY 10000TL-US Inverter Datasheet Page 1

Technical data	Sunny Boy 8000TL-US	Sunny Boy 9000TL-US	Sunny Boy 10000TL-US
	208 V AC	208 V AC	208 V AC
Input (DC)			
Max. recommended PV power (@ module STC)	10000 W	11250 W	12500 W
Max. DC power (@ cos φ =1)	8400 W	9400 W	10500 W
Max. DC voltage	600 V	600 V	600 V
DC nominal voltage	345 V	345 V	345 V
MPP voltage range	300 V - 480 V	300 V - 480 V	300 V - 480 V
Min. DC voltage / start voltage	300 V / 360 V	300V / 360 V	300 V / 360 V
Max. input current / per string (at DC combiner box)	28 A / 28 A	31 A / 31 A	35 A / 35 A
Number of MPP trackers / fused strings per MPP tracker	1 / 6 (@ Combiner Box)	1 / 6 (@ Combiner Box)	1 / 6 (@ Combiner Box)
Output (AC)			
AC nominal power	8000 W	9000 W	10000 W
Max. AC apparent power	8000 VA	9000 VA	10000 VA
Nominal AC voltage / adjustable	208 V / –	208 V / –	208 V / –
AC voltage range	183 V - 229 V	183 V - 229 V	183 V - 229 V
AC grid frequency; range	60 Hz; 59.3 - 60.5 Hz	60 Hz; 59.3 - 60.5 Hz	60 Hz; 59.3 - 60.5 Hz
Max. output current	40 A	44 A	49 A
Power factor (cos φ)	1	1	1
Phase conductors / connection phases	1 / 2	1 / 2	1 / 2
Harmonics	< 4%	< 4%	< 4%
Efficiency			
Max. efficiency	98.3%	98.3%	98.3%
CEC efficiency	98%	98%	97.5%
Protection devices			
DC reverse-polarity protection	●	●	●
AC short circuit protection	●	●	●
Galvanically isolated / all-pole sensitive monitoring unit	–/●	–/●	–/●
Protection class / overvoltage category	I / IV	I / IV	I / IV
General data			
Dimensions (W / H / D) in mm (in)	470 / 615 / 240 (18.5 / 24 / 9)		
DC Disconnect dimensions (W / H/ D) in mm (in)	187 / 297 / 190 (7 / 12 / 7.5)		
Packing dimensions (W / H / D) in mm (in)	390 / 580 / 800 (16 / 23 / 31.5)		
DC Disconnect packing dimensions (W / H / D) in mm (in)	370 / 240 / 280 (15 / 9 / 11)		
Weight / DC Disconnect weight	35 kg (77 lb) / 3.5 kg (8 lb)		
Packing weight / DC Disconnect packing weight	40 kg (88 lb) / 4 kg (9 lb)		
Operating temperature range / full power range	-25 °C ... +60 °C (-13 °F ... +140 °F) / -25 °C ... +45 °C (-13 °F ... +113 °F)		
Noise emission (typical)	≤ 46 dB(A)	≤ 46 dB(A)	≤ 46 dB(A)
Internal consumption at night	≤ 0.25 W	≤ 0.25 W	≤ 0.25 W
Topology	transformerless H5	transformerless H5	transformerless H5
Cooling concept	OptiCool	OptiCool	OptiCool
Electronics protection rating / connection area	NEMA 3R / NEMA 3R	NEMA 3R / NEMA 3R	NEMA 3R / NEMA 3R
Features			
Display: text line / graphic	●/–	●/–	●/–
Interfaces: RS485 / *Bluetooth*	○/○	○/○	○/○
Warranty: 10 / 15 / 20 years	●/○/○	●/○/○	●/○/○
Certificates and permits (more available on request)	UL1741, UL1998, IEEE 1547, FCC Part 15 (Class A & B), CSA C22.2 No. 107.1-2001		
NOTE: US inverters ship with gray lids.			
● Standard features ○ Optional features – Not available			
Revised August 2010 Data at nominal conditions			
Type designation	SB 8000TLUS-10	SB 9000TLUS-10	SB 10000TLUS-10

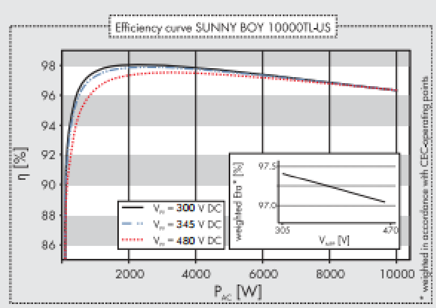

Accessories

Sunny Boy Combiner Box
SBCBTL6-10
(Included with inverter)

Bluetooth® Piggy Back
BTPBINV-NR

RS485 interface
485USPB-SMC-NR

SMA Power Balancer
PBL-SBUS-10-NR

Toll Free +1 888 4 SMA USA
www.SMA-America.com

SMA America, LLC

Figure F-2: SMA SUNNY BOY 10000TL-US Inverter Datasheet Page 2

Appendix G

ABB Single Phase Overhead Distribution Transformer

Figure G-1: ABB Single Phase Overhead Distribution Transformer Datasheet Page 1

Product overview

Application

The ABB overhead transformer may be used alone for the supply of a single phase load or as one of three units in a bank for the supply of a three phase load. The unit may be direct-mounted to a wooden or concrete pole, or cluster mounted on a pole for three phase use. The ABB transformers are designed for servicing residential overhead distribution loads. They are also suitable for light commercial loads, industrial lighting and diversified power applications.

Standards

All units are built in accordance with both CAN CSA C2.1-06 and CAN CSA C2.2-06, except as modified to comply with customer specifications. IEEE C57.12.20 or International Electrotechnical Commission Standard (IEC) may apply if required.

Features

- Core and coils designed for an optimum Total Ownership Cost (TOC)
- Wound core with step-lap joints for increased efficiency and lower noise levels
- "Low-high-low" windings for increased short circuit strength, efficiency and thermal strength
- Computer aided design for mechanical & electrical calculations (C.A.D.)
- Dual voltage designed to meet BIL and short circuit requirements on both connections
- Low voltage leads with embossed markings on all units with 3 LV bushings for easy reading and permanent identification on selected ratings
- Paint system meeting or exceeding the performance of the IEEE C57.12.28 Standard (para. 5.3 to 5.5 included), including the salt spray test
- Lifting lugs meeting all of the requirements of the CSA C2.1-06 and CSA C2.2-06 Standard (including feature to prevent sling slippage)
- Multiple cover clamps to ensure proper sealing and to minimize water retention on the cover edge
- Cover or sidewall mounted high voltage bushing(s) as required
- Low voltage spade or clamp type (basket) terminals as required
- Provision for surge arrester bracket, bracket available as an option
- Automatic self-resealing pressure relief valve

Dual Voltage Transformers and Taps

Dual voltage transformers have proven to be very useful for their versatility which allows lower inventories for the electric utilities and saves on change out costs in the event of upgrading to higher system voltage. Because taps are also in common use, it is appropriate that dual voltage transformers with taps be considered. As the transformer reliability is adversely affected by the increased number of HV leads introduced by dual voltage designs, ABB recommends the following:

- Dual Voltage transformers without taps should be limited to a 4:1 ratio (eg 2.4 x 8.0 kV)
- If taps are required on both connections, the voltage ratio should be 2:1

Accordingly, ABB recommends that:

(1) dual voltage transformers without taps be limited to a maximum HV spread of 2400V x 8000V, or 4800V x 16000V, and that

(2) transformers with taps (for both connections) be limited to a maximum spread of 2.1, for example 7200V x 14400V, or 8000V x 16000V.

Pole Mounted Transformers, Rating Details

General technical information is listed below. Information on less common requirements can be obtained through your ABB sales representative.

- kVA: 10, 15, 25, 37, 50, 75, 100, 167
- Temperature rise : 65 °C
- Cooling type : ONAN
- Single Phase
- Hertz : 60, 50
- Polarity : Additive or Subtractive
- Primary Voltage : 2400V through 34500 GrdY / 19920V
- Secondary Voltage : 120 / 240V, 240 / 480 V, 347V, 600V
- Insulation Class : 25kV (150kV BIL) and below
- Taps: none, or as an option, 4 x 2,5% HV (any combination of full capacity above nominal and /or reduced capacity below nominal)

Options

- Four HV winding taps complete with externally operated tapswitch
- Dual voltage primary complete with externally operated voltage switch
- Extra creep bushing
- Surge arrester bracket
- Internal Fault Detector (IFD)
- Non conductive transformer cover
- Biodegradable vegetable oil (BIOTEMP®)
- Stainless steel tank and cover

2 Single phase overhead distribution transformers

Figure G-2: ABB Single Phase Overhead Distribution Transformer Datasheet Page 2

Outline Drawings

The influence of the loss evaluation formulae on transformer designs will lead to a wide variety of sizes and weights, thereby making it difficult, for the purpose of this information sheet, to cover the broad range of dimensions.

Typical Dimensions (mm) for grain oriented electrical design

KVA	A	B	C	D	Mass (kg)	Oil (litres)
10	885	560	500	525	100	22
25	935	610	560	590	160	30
50	1035	710	635	675	260	60
75	1035	710	745	840	375	90
100	1135	815	770	965	555	100
167	1335	1015	795	890	690	160

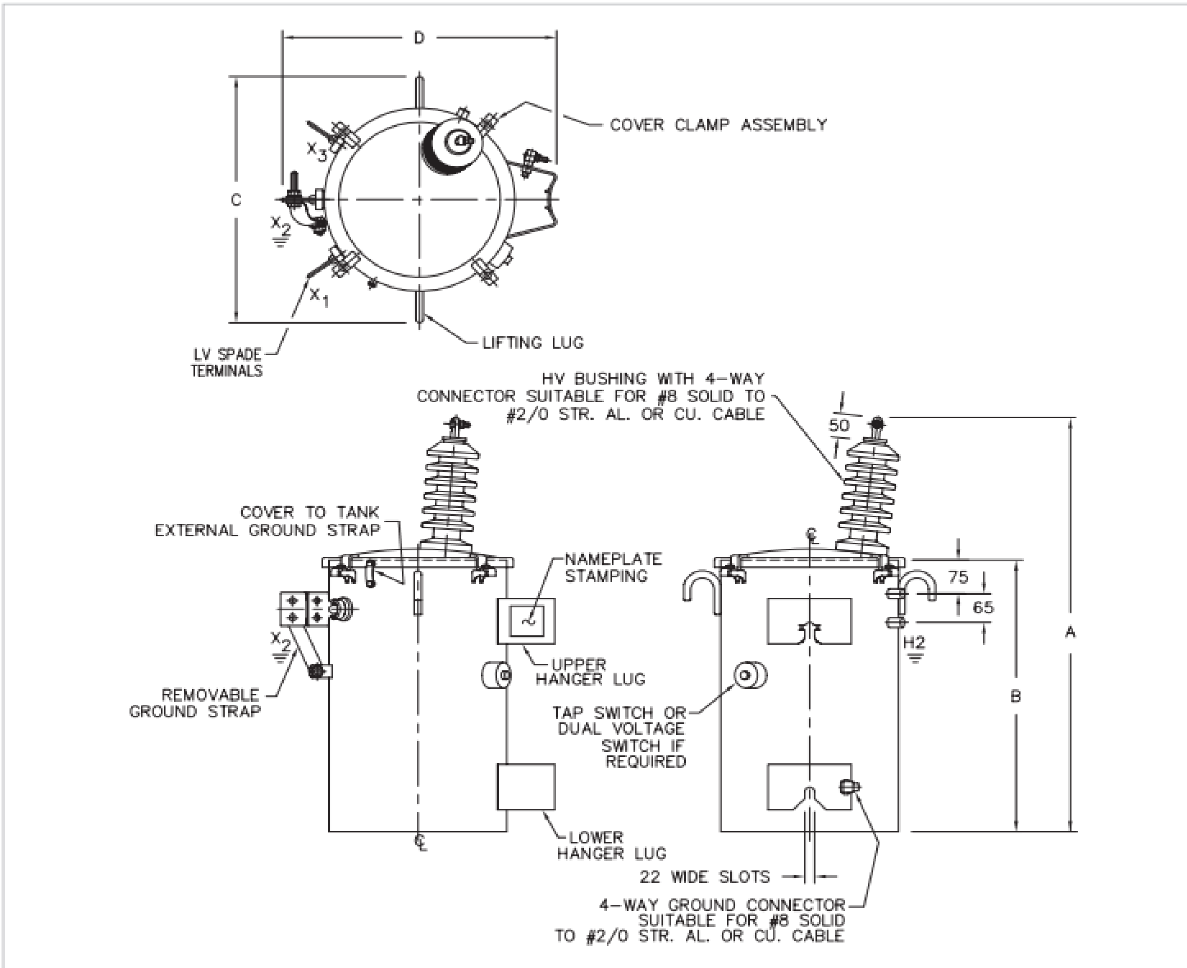

Single phase overhead distribution transformers 3

Figure G-3: ABB Single Phase Overhead Distribution Transformer Datasheet Page 3

Appendix H

proportional and integral terms

In this appendix the constant control values are shown in the table below.

Unit	Power Electronics Device	Control	Ki_1	Kp_1	Ki_2	Kp_2
ESS	Bidirectional-Converter	Voltage / Flow Power	5	2	0.04	0.5
PV	Boost-converter	MPPT	1	0.45	-	-

Where Ki_1 and Kp_1 are the terms of the outer loop, instead Ki_2 and Kp_2 are related to the inner loop.